5-2023

Investigation the Plugging Behavior of Virus filters

Iman Abdulqader Saab
University of Arkansas-Fayetteville

Investigation the Plugging Behavior of Virus filters

A thesis submitted in partial fulfillment
of the requirements for the degree of
Master of Science in Cell and Molecular Biology

by

Iman Abdulqader Saab
Tikrit University
Bachelor of Education in Biology Science, 2010

May 2023
University of Arkansas

This thesis is approved for recommendation to the Graduate Council.

Xianghong Qian, Ph.D.
Thesis Director

Ranil Wickramasinghe, Ph.D.
Committee Member

Robert Beitle Jr., Ph.D.
Committee Member

Abstract

A virus filtration step is integral to the manufacturing of biopharmaceuticals to ensure viral safety. A virus filter is a single-use device that uses a size-based separation process and has a unique structure with minimal defects, so that contaminating virus particles cannot pass through the membrane pores, while therapeutic molecules can. The development of novel antibodies (Abs), including significant increases in product titers, is frequently challenged by virus filter fouling, making a better understanding of the underlying mechanisms essential. This thesis focused investigating of the effect of prefilter types, buffer type and salt content on virus filtration performance. The impact of the protein-protein interactions and their aggregates on the filtrate flux during virus filtration of highly concentrated mAb solutions are also investigated.

In Chapter 2, prefiltration and flux decay studies were performed with a different concentration of polyclonal human immunoglobulin G (IgG) using two commercially Prefilters (Viresolve® pre-filter and Planova 75N) and virus filters (Viresolve® Pro and Planova BioEx). The fouling behaviors of the virus filters were strongly affected by the concentration of the feed solution and protein oligomers. The prefilters did not provide much benefit in improving the filtrate flux at high concentrations. Filtration using Planova BioEX in two runs without prefiltration shows less fouling and significant flux improvement in the second run and the application of post-filtration buffer flush with different conditions results in higher flux recovery in the second run than the first run. Size exclusion chromatography (SEC) analysis for IgG solution in different buffer conditions revealed that the aggregate concentration increases slightly as the IgG concentration increases. Results using dynamic light scattering (DLS) in the same buffer conditions shows that the mean hydrodynamic diameter increases as the increase of protein concentration and the protein tends to have attractive interactions in both buffer conditions. This IgG has a high molecular weight (250 kDa) and it is moderately hydrophobic.

In Chapter 3, virus filtration was performed with an industrially monoclonal antibody (mAb C) with different concentrations up to 50 g/L in different buffer conditions using Viresolve Pro virus filter and adsorptive prefilters. This mAb was subjected to decoupled prefiltration to evaluate how different types of prefilters affected its filterability. Filter fouling is found to be strongly affected by the product concentration and the presence of aggregates. An analysis of size exclusion chromatography (SEC) showed that the presence of large amount of high molecular weight species considered as irreversible aggregates correlates with irreversible fouling that caused reduced mAb throughput and filter fouling. Results using dynamic light scattering (DLS) in different buffer conditions shows that the mean hydrodynamic diameter increases as the increase of protein concentration and the protein tend to have a stronger tendency to aggregate in tris buffer compared to sodium phosphate buffer. The pharmaceutical analysis system PA800 plus was also used to characterize the various mAb fractions from prefiltration and virus filtration.

In Chapter 4, an overall conclusion for this work showing major findings and identifying areas for future study.

Acknowledgements

I would like to thank my supervisor Prof. Xianghong and my co-advisor Prof. Ranil Wickramasinghe for supporting me during my research to complete this degree successfully. I would also like to thank all the current and former group members of the Qian research group and the Wickramasinghe research group (Drs. Ronny Horax, Xiaolei Hao, Solomon Ogbonnia Isu and Wenbo Xu), who made my research and life enjoyable. I am grateful for all the helpful advice, collaborations, and discussions.

I want to thank the industry advisory board of the MAST Center for funding my M.S. research and providing astute mentors to guide my research.

I would like to thank my family for their support and encouragement, especially my parents and my husband Mahmood Jebur, my children, Yahya and Yousif. You have all been a source of strength and a pillar of support.

Table of Contents

List of Figures

List of Tables

List of Equations

CHAPTER 1: General Introduction

1.1 Production of Biotherapeutics

The recombinant DNA technology has led to successful formulation of many protein therapeutics in the last two decades (Shire et al., 2004). Researchers have developed protein therapies for a wide variety of diseases, including AIDS, hepatitis, diabetes, arthritis, hemophilia, multiple sclerosis, cancer, infectious disease, cardiovascular disorders, etc. (Dimiter, 2012). Among the first products derived from recombinant proteins were highly active hormones, cytokines, and clotting factors such as insulin. In 1982, the FDA approved the first commercial recombinant human therapeutic, human insulin (Carter, 2011). Most of these bioproducts were used at relatively low doses, and less than 1 kg was produced each year (Zydney, 2009).

Most biopharmaceuticals products are created by using several expression systems. Recombinant proteins are expressed in a variety of hosts, including bacteria, mammalian cells, yeast, insect cells, animals, and plants that are transgenic (McKenzie & Abbott, 2018; Owczarek et al., 2019; Puetz & Wurm, 2019; Tripathi & Shrivastava, 2019). Escherichia coli can produce a high yield with a fast growth rate. Yeast expression system (*Saccharomyces cerevisiae and Pichia pastoris*) can give post-translational modifications (PTMs). Mammalian cell lines are the favored method of production all approved recombinant therapeutics. Today, the cell-free protein synthesis method is gaining more attention because it produces complex proteins, it is not restricted by homeostasis conditions to maintain cell viability, and it can save time and effort by eliminating complicated and costly steps such as gene transfection, cell culture, and extensive protein purification (Kesik-Brodacka, 2018; Shinoda et al., 2016).

The US Food and Drug Administration (FDA) approved 29 monoclonal antibodies (mAbs) in 2009, which accounted for 35 percent of the total biologics market (Aggarwal, 2009;

Rosenberg, 2010). Most of them belong to the immunoglobulin isotype G (IgG) and the subclass IgG1 (Nissim & Chernajovsky, 2008). A human recombinant IgG1 antibody (Adalimumab (Humira)) inhibiting tumor necrosis factor alpha was approved in 2006 as the first recombinant IgG1 antibody. The phage-display technology was used to generate specific antibodies from human antibody gene repertoires in vitro (Winter et al., 1994).

In the biopharmaceutical industry, monoclonal antibodies (mAbs), peptides and recombinant proteins make up the majority of new products in development (Dumont et al., 2016). Recently, the development of mAbs products has gained a lot of attention due to their high target specificity in selectively binding to the target cell or molecule. The production of some mAbs can be as large as 1000 kg in a typical year, whereas hormones, which act as catalysts, need much lower dosing levels, and batch sizes (Binabaji, 2015). As a result, mAbs have quickly emerged as the most popular class of new medicines for pharmaceutical companies. Their market share grew to 115.2 billion dollars in 2018 and is expected to reach nearly 300 billion dollars by 2025 (Liu, 2014). It has been established that mAb products will meet standards of quality, efficiency, and safety that will enable them to be successfully commercialized and approved, resulting in a greater chance of clinical success and a reduction in the time necessary for their development (Reichert, 2008).

The difficulty in achieving the High final concentrations is one of the challenges in production of mAb products for the industry. In most cases, mAb are given frequently and in large doses (characterized as mg mAb/kg patient body weight) (Shire et al., 2004). The pharmaceutical industry is increasingly focusing on high protein concentrations (>50 mg/mL) in aqueous compositions. To deliver high doses in small amounts, mAb should be formulated at high concentrations (Jezek et al., 2011). It is likely that higher levels of concentrations will occur

in the future, about 100-200 g/L, due to the limited quantity of injectable solution that can be delivered via subcutaneous injection (SC) (1-2mL). In intravenous (IV) immunoglobulin therapies, polyvalent immunoglobulins pooled from healthy blood donors also require high antibody concentrations (Burckbuchler et al., 2010). These treatments are effective both as a replacement therapy and as a modulator of various autoimmune or inflammatory diseases (Emmi & Chiarini, 2002).

mAbs are a group of large multimeric proteins (approximately 150 kDa) consisting of pairs of heavy and light chains associated with disulfide bonds (Buss et al., 2012). The correct glycosylation pattern and three-dimensional structure of mAbs is generally obtained using mammalian cell lines (Binabaji, 2015). The first mAb was created in 1975 when Kohler and Milstein combined murine myeloma cells with murine-antibody-secreting lymphocytes. Since that time, many more mAbs have been created and used for various purposes, for example, symptomatic strategies and immunotherapy (Berger et al., 2002; Kamusheva et al., 2021). Between 1980 and 2005, 206 different therapeutic mAbs were studied in clinical trials, with 12 anticancer mAbs were approved for commercial use (Reichert & Valge-Archer, 2007). At present, more than 360 mAbs are being studied in clinical trials, including 30 pivotal trials. Over 30 mAb therapeutics have already been approved for use in humans (Reichert, 2013).

1.2 Downstream purification

There are typically two main steps in biopharmaceutical manufacturing: an upstream process that uses cell culture for expression of the targeted product, and a downstream process that separates the upstream mix from the downstream mixture (Isu et al., 2022; Papathanasiou et al., 2017).

There is a risk of safety and efficacy issues with the production of mAbs due to the presence of both product-related impurities like aggregates, fragments, oxidized or deaminated species and process-related impurities like Host Cell Protein (HCP), Retrovirus-Like Particles (RVLP), leachates, and reaction byproducts (Chon & Zarbis-Papastoitsis, 2011; Sommerfeld & Strube, 2005). Today's biopharmaceutical industry faces major challenges such as reducing impurities and processing time, while still achieving high end-concentrations (Marichal-Gallardo & Álvarez, 2012). The high purity needed for mAbs products is achieved through several unit operations which have different separation mechanisms and capacities, each removing different classes of impurities.

Figure 1.1 Shows a schematic diagram of a platform process for the downstream purification of mAbs. In the initial step of downstream processing, the batch medium in which cells secrete mAbs is centrifuged to remove the cell debris and other large particulates, and the supernatants are harvested. The next step is to run the supernatant through two purification processes, Protein A chromatography is applied as a capturing step which involves hydrophobic interactions between the protein A ligand and the crystallizable fragment region (Fc region) of the antibody's heavy chain (Zhang et al., 2019). The capture pool of mAb purification typically contains small amounts of impurities once the target protein has been captured. The next step is to complete the purification process. In most mAb manufacturing processes Protein A affinity chromatography is followed by two additional chromatography polishing steps such as hydrophobic interaction chromatography (HIC) and ion-exchange chromatography (IEX) (comprising cation exchange chromatography (CEX) and anion exchange chromatography (AEX)) to remove the remaining impurities and product aggregates (Chollangi et al., 2015). Contaminants and aggregates are separate by IEX chromatography according to their charge

characteristics. The chromatographic media contains oppositely charged groups that interact with charged groups on a protein. A protein's charge is determined by its environment's pH. In AEX chromatography, negatively charged impurities such as host cell proteins and DNA are removed by binding to positively charged functional groups. CEX chromatography is effective in removing host cell DNA, HCP, and protein aggregates by using negatively charged functional groups.

Based on differences in hydrophobicity in the presence of buffer salts, HIC polishing is highly effective for removing aggregates and denatured proteins (Rosenberg, 2010). By using size exclusion chromatography (SEC), it is possible to separate impurities according to their different molecular weights. It is generally utilized as a polishing step to remove antibody aggregates and fragments with a large range of sizes. As part of this technique, a gel is packed into a chromatographic column in an aqueous buffer solution. Biomolecules diffuse through this gel based on their molecular size differences, which are composed of spherical porous particles with carefully controlled pore sizes (Fekete et al., 2013; Sommerfeld & Strube, 2005).

A highly purified, moderately concentrated product is created near the end of the purification train by Virus filtration. When product concentrations reach high levels, aggregation and adsorption can compromise virus filter performance. The final step in the purification process is ultrafiltration or diafiltration to achieve the desired product concentration and to separate proteins from buffer components for buffer exchange (Leenaars & Hendriksen, 2005; Nielsen, 2022).

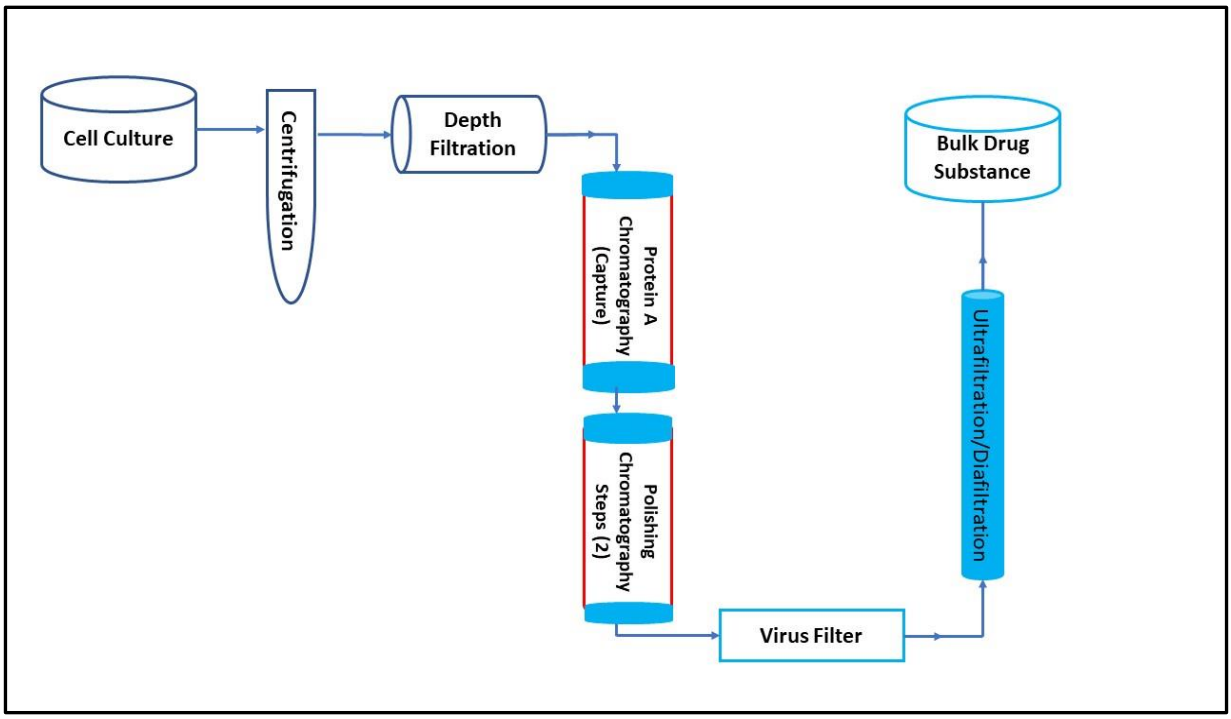

Figure 1.1 Basic process flow for the production of mAbs (Nielsen, 2022).

Today, it is extremely difficult to create and scale up purification systems that can generate kilogram amounts of purified mAb at the lowest feasible cost because of the ability to produce multiple kilogram quantities of mAb each batch through large-scale cell culture techniques (Sommerfeld & Strube, 2005). Higher concentrations (and correspondingly lower volumes) of intermediate solutions obtained through downstream processing are advantageous because they are simpler to handle and store (Rao et al., 2012). However, a range of formulation and handling issues have been met with these highly concentrated antibody products because of their high viscosity, protein instability, and very low filtrate flux (Harris et al., 2004; Rao et al., 2012).

1.3 Membranes in Downstream Purification

Membrane processes are play a significant role in various applications in the field of separation/purification of the earliest biotechnological products. In the past, they were used

for separating biomolecules long before the modern membrane industry began. Because of their unique properties, high throughput, scalability, mild conditions, and cause little degradation of high value biomaterials, these processes are well suited to the biotechnology industry. The biotechnology industry has developed new membranes and modules over the last two decades (Howell et al., 1993; Saxena et al., 2009; van Reis & Zydney, 2007).

There has been widespread interest in the applications of the pressure-driven processes of ultrafiltration, microfiltration, and virus filtration. The most downstream bioprocesses used in biopharmaceutical and pharmaceutical manufacturing is virus filtration, also known as nanofiltration, to remove viruses from the process stream by size exclusion (Wickramasighe et al., 2019). In contrast to typical pressure-driven membrane filtration processes, virus filter is designed to achieve extremely high levels of elimination for virus contaminants. Further, since it is impossible to confirm there is no carryover of any trapped virus particles, virus filters cannot be reused. Virus filtration membranes are one time use only and operate in normal flow mode (dead end). Since normal flow (dead end) mode is less complex and requires only a single pump, virus filters are typically run in this mode rather than tangential flow mode, which is used for protein ultrafiltration (Bohonak & Zydney, 2005; Isu et al., 2022).

As shown in Table 1.1, membrane materials used in virus filters are typically regenerated cellulose, polyvinylidene difluoride (PVDF), and polyethersulfone (PES). The latter materials are naturally hydrophobic and are modified to be more hydrophilic to reduce the levels of protein adsorption, fouling, and product denaturation during virus filtration. A membrane structure can be single or multilayer flat sheet membranes, and they can also be hollow fibers with symmetric or asymmetric structure. Asymmetric membranes for virus

filtration have an open surface that faces the feed, unlike ultrafiltration membranes (Bakhshayeshi & Zydney, 2008; Gefroh et al., 2014). These virus filters have been designed to remove nonenveloped parvoviruses that are between 18 and 26 nm and enveloped retroviruses that are larger than 80nm (Wickramasighe et al., 2019). Previously, retrovirus and parvovirus removal filters were included in the purification train (FDA, 1997). Virus clearance filters that are designed to remove smaller parvoviruses can also remove much larger retroviruses at the same time as indicated by recent research (Miesegaes et al., 2014). Additionally, these virus filters can pass only monomers biomolecules with a hydrodynamic diameter less than 20 nm through the pores of the filters (Robinson et al., 2018).

Virus filtration membranes are currently ultrafilters or very tight microporous filters, and their pore size ratings vary depending on the vendor. Operating pressures and permeate fluxes also differ significantly. The pore size distribution is among the most crucial factors in a virus filter because of its relationship to virus retention, filtrate flux, and overall protein yield. Integrity tests are performed on filters to identify oversized pores or defects that can impair their retention capability (Giglia & Krishnan, 2008).

Table 1.1 Commercially Available Virus Filters (Gefroh et al., 2014; Isu et al., 2022; Johnson et al., 2022).

Filter Brand	Manufacturer	Membrane Chemistry	Pore symmetry and format	Comments
Viresolve NFR	MilliporeSigma	Polyethersulfone	Asymmetric triple-layer pleated sheets	Retrovirus filter
Viresolve Pro	MilliporeSigma	Polyethersulfone	Asymmetric triple-layer pleated sheets	Parvovirus filter
Planova 15 N, 20 N	Asahi Kasei Bioprocess	Regenerated cellulose	Asymmetric single-layer hollow fibers	Parvovirus filter
Planova 35 N	Asahi Kasei Bioprocess	Regenerated cellulose	Asymmetric single-layer hollow fibers	Retrovirus filter
Planova BioEX	Asahi Kasei Bioprocess	Hydrophilized PVDF	Asymmetric single-layer hollow fibers	Parvovirus filter
Virosart HC	Sartorius AG	Polyethersulfone	Asymmetric double-layer pleated sheets	Parvovirus filter
Virosart HF	Sartorius AG	Modified polyethersulfone	Asymmetric single-layer hollow fibers	Parvovirus filter
Pegasus SV4	Pall Corporation	Hydrophilized PVDF	Symmetric double-layer pleated sheets	Parvovirus filter
Pegasus Prime	Pall Corporation	Polyethersulfone	Pleated sheets	Parvovirus filter
Ultipor VF DV20	Pall Corporation	Hydrophilized PVDF	Symmetric double-layer	Parvovirus filter

1.4 Virus Filter Fouling and flux decay

In the manufacturing of biopharmaceuticals, fouling of virus filter membranes is a significant issue (Bieberbach et al., 2019; Bolton et al., 2010; Rayfield et al., 2015). Fouling can reduce membrane capacity, which is defined as how much filtrate can be collected before the filtrate flux decreases to an unacceptable level (Kosiol et al., 2019). Physical and chemical

characteristics of membrane and protein solutions, such as electrostatic interactions, are important factors for determining the performance of filtration (Syedain et al., 2006). Using the highly asymmetric Viresolve Pro filter, Billups et al. (2022) demonstrated that orienting the filter with the skin side down decreased filtrate flux by about 10-fold but orienting it with the skin side up reduced flux by more than 1000-fold. In order to maximize filter capacity, it is also necessary to establish the best processing parameters and the best operation mode such as continuous flow or constant pressure. Several research (Dishari et al., 2015; Willkommen et al., 2013; Woods & Zydney, 2014) have shown that utilizing a low operation pressure or halting the process might lower the capacity of a viral filter.

In most cases, virus filtration takes place just prior to the downstream purification step, so the process stream consists mostly of the protein of interest and very little contamination or virus. As a result, most virus filters will be fouled by the deposition of protein products rather than virus particles and their aggregates on the surface and inside the pores of the membrane, given the high level of product concentration at the end of the purification train. (Bohonak & Zydney, 2005; Lutz et al., 2011; Troccoli et al., 1998). Several early studies (Belfort et al., 1994; Kelly & Zydney, 1994) have suggested that the interactions between virus membranes and proteins are one of the major causes of initial fouling.

Many factors can cause therapeutic mAbs to aggregate, including long-term storage at moderate or high concentrations, chemical degradation, interactions with excipients and physical stresses (Shieh & Patel, 2015). A tendency for therapeutic mAbs to aggregate is a concern because such aggregation can affect the quality, potency, safety, and immunogenicity of the product (Kessler et al., 2006; Rosenberg, 2006). According to earlier research, molecular size determined by absolute size exclusion chromatography is an important determinant of virus

filtration performance (Rayfield et al., 2015). They found that aggregates bigger than 17 nm were correlated to the flux decline during virus filtration. Bieberbach et al. (2019) classified aggregates into two groups by analyzing the feed stream of virus filters: reversible aggregates and irreversible aggregates. They have also observed that irreversible aggregates cause continuously increasing pore clotting and continuously decreasing flux. These irreversible aggregates can be removed using hydrophobic prefilters. On the other hand, when reversible aggregates form, they cause reversible fouling, resulting in a concentration dependent initial flux decay with no further flux decline. Dilution of the feed can mitigate these flux reductions but only when there is a high product titer in the solution. While the extent of the risk that aggregates pose remains unclear, it is critical to identify mAb candidates with a tendency to aggregate during development so that appropriate risk mitigation strategies can be implemented (Rosenberg et al., 2012; Singh et al., 2010).

Several physical stresses can also be applied to proteins and affect the stability of a monomer throughout manufacturing, including air-liquid interfaces, solid surfaces of hydrophobic and hydrophilic materials, and temperature variations which induces nucleation and aggregation (Shieh & Patel, 2015). Product freezing and thawing causes more aggressive fouling of virus filters (Barnard et al., 2014; Isu et al., 2022; Wickramasighe et al., 2019). Aggregation is caused by conformational changes at the ice-water interface as well as freeze concentration (Kueltzo et al., 2008; Manning et al., 2010). Moreover, different chemical stresses such as pH changes, ionic strength changes, and buffer species changes. Adding salts to a protein solution can alter their conformational stability as well as the colloidal stability of the system, while pH and ionic strength influence the electrostatic repulsion between the protein, thus affecting protein self-association (Bakhshayeshi & Zydney, 2008; Namila et al., 2019; Rosenberg, 2010).

At the isoelectric point (pI) of the product, aggregation and precipitation occur more readily due to reduced electrostatic repulsion between individual product molecules. In early studies showed that Viresolve® 180 for BSA the lowest membrane capacity at the protein isoelectric point (pI), with increases monotonic as pH increased above the pI (Bakhshayeshi & Zydney, 2008; Novák & Havlíček, 2016).

1.4.1 Mitigation of Virus Filter Fouling

The technique of virus filtration offers a robust, size-based approach to the removal of viruses through the production of biopharmaceutical products. Virus filters are designed to remove a very high level of potential impurities due to their unique structure and selective pore that are only slightly larger than proteins. Prefilters can greatly enhance the performance of parvovirus filters, and by analyzing the species entrapped in the prefilter, it is possible to gain insight into how virus filters foul (Bolton et al., 2010; Ireland et al., 2005).

Virus filters are often used in-line with prefilters to improve throughput and reduce cost. These prefilters remove trace impurities that could otherwise foul virus filters, thus reducing area requirements and increasing throughput (Bolton et al., 2006; Brown et al., 2010). Today, most virus filter manufacturers offer specialized prefilters in order to increase the capacity and throughput of their virus filters. Table 1.2 includes some examples of common prefilter options. Using the Viresolve® Prefilter developed by MilliporeSigma (Bolton et al., 2006), more than a 10-fold improvement was observed in the filtration capacity of serum IgG through the Viresolve® NFP virus filter, compared with other prefilters. It was determined that the large increase in capacity was a result of the removal of monomeric hydrophobic variants of IgG from the Viresolve® Prefilter, which were probably bound to diatomaceous earth. PlanovaTM 20N, Viresolve® Pro, and Virosart® CPV have been shown to have improved mass throughput when

combined with a depth filter A1HC and a virus filter, Viresolve® Pro, which was used as a size-based pre-filter (Bolton et al., 2010).

Several commercial membrane adsorbers developed for the purification of mAbs such as Sartobind® S and Q which is a separate unit operation (not inline) that adsorbs negatively charged proteins, DNA, and viruses from host cells. As reported by Brown et al. (2010), adsorptive ion exchange membrane prefiltration can enhance parvovirus filter throughput of mAbs by binding trace foulants and some antibody products. Additionally, ion exchange membranes facilitate characterization of parvovirus filter foulants. Prefilters with hydrophobic property require a moderate/high salt content (ionic strength) to reduce the soluble layer of the product, enabling exposed hydrophobic patches to bind with the prefilter. The use of hydrophobic interaction prefilters may be effective in removing some of the more hydrophobic product aggregates, as well as variants with different hydrophobicity (Isu et al., 2022).

In addition, microfiltration membranes with pores of 0.1 to 0.22 µm are also used as prefilters for virus filtration to remove aggregates larger than the size cut-off of the prefilter. However, researchers have previously shown that the size range of the foulants on virus filtration membranes is around 16-40 nm (Barnard et al., 2014; Rayfield et al., 2015).Therefore, the foulants cannot be completely removed by microfiltration prefilters. The results of study by Brown et al. (2010) indicate that size-based pre-filters such as 0.1 and 0.22 µm are largely ineffective, and depth filters are generally more reliable but exhibit lower stability in caustic environments, leading to higher leachable.

Table 1.2 Common Commercially Available Prefilters (Gefroh et al., 2014; Isu et al., 2022; Johnson et al., 2022).

Prefilter Brand	Manufacturer	Membrane Chemistry	Mechanism of Action
Viresolve® Shield	MilliporeSigma	Surface modified PES	Ion exchange (cation) and Size exclusion
Viresolve® Shield-H	MilliporeSigma	Surface modified PES	Hydrophobic interaction and Size exclusion,
Viresolve® Prefilter	MilliporeSigma	Composed of diatomaceous earth, cellulose fibers and abinder containing cationic imine groups	Cation exchange, size exclusion, hydrophobic interaction, ion exchange
Planova 75 N	Asahi Kasei Bioprocess	Regenerated cellulose	Size exclusion, removal of small aggregates
Bottle top 0.1, 0.22 µm	Multiple	Polyethersulfone	Size exclusion, removal of large aggregates
Pegasus Protect	Pall Corporation	Nylon	Size exclusion, removal of large aggregates
Sartobind Q	Sartorius AG	Quaternary ammonium ligands	Anion exchange
Sartobind S	Pall Corporation	Sulfonic acid ligands	Cation exchange
Sartobind phenyl	Pall Corporation	Phenyl ligands	Hydrophobic interaction

1.5 Protein Characterization Techniques

Pharmaceutical companies are increasingly approving mAbs, and biosimilars may enter the market in the near future, which has resulted in the need for analytical techniques that can accurately characterize these proteins. Since differences in impurities and/or degradation products may have serious health consequences, the intrinsic micro-heterogeneity of mAbs needs to be carefully assessed to ensure the quality and safety of drug product. Molecular properties, charge and hydrophobicity variants are usually identified during the development process via physicochemical characterization techniques (Fekete et al., 2013; Thiagarajan et al., 2016). One

of the essential characteristics in assessment studies is size variations since size distribution or monodispersity of a mAb product is important for both safety and efficacy. Components larger than the individual antibody can cause size-related heterogeneity due to association, aggregation, or precipitation. It is possible that a mAb preparation contains a wide range of species, from molecular dimers to oligomers to higher-order aggregates (Fekete et al., 2014). It is well documented in the literature that Size Exclusion Chromatography (SEC), Ion Exchange Chromatography (IEX), and Hydrophobic Interaction Chromatography (HIC) are theoretically and practically equivalent (Fekete et al., 2014; King et al., 2018). It has been found that SEC can be applied to both native and denatured antibodies to determine the high molecular weight species (HMWS) and separate them according to their molecular size into three major species: high molecular weight species (HMWS), main peak (predominantly the monomeric form), and low molecular weight species (LMWS) (Goyon et al., 2017). IEX consists of two subtypes: cation exchange chromatography (CEX) and anion exchange chromatography (AEX). Proteins are eluted through salt gradients or pH gradients (Kahle et al., 2019). Dynamic Light Scattering (DLS) can be utilized as an additional technique for the general characterization of proteins. The method is relatively fast, requiring only a few minutes to quantify the size of biomolecules in solution, with high sensitivity towards small quantities of aggregates and user-friendly software. DLS is capable of determining whether a sample is homogeneous monodisperse or aggregated, however it does not have the ability to separate monomer from aggregates but computes the average size of the particles in the sample instead. The intensity or fluctuations of scattered light may be analyzed either as an indicator of intensity or as an indicator of fluctuations when light passes through a solution containing molecules. Intensity data captured by DLS can be used to

estimate diffusion coefficients and hydrodynamic radiuses of molecules (Bansal et al., 2019; Nobbmann et al., 2007).

Traditionally, Sodium Dodecyl Sulfate (SDS) Polyacrylamide Gel Electrophoresis (PAGE) has been used for the molecular weight (MW) determination of proteins by separating them based on their size and purity, which ensures they have the same mass/charge ratio and migrate in the same direction at different rates. Due to the drawbacks associated with SDS-PAGE assays, such as long analysis times, low efficiency, limited reproducibility, and use of toxic reagents, many biopharmaceutical laboratories have begun developing Capillary Electrophoresis–SDS Molecular Weight (CE-SDS MW) gels instead (Rustandi et al., 2008; Wiesner et al., 2021). It is evident that CE-SDS gel has numerous advantages over SDS-PAGE, including automation, reproducibility, robustness, resolution, and speed. CE-SDS has also been found to be more accurate in quantitating low molecular weight species (LMWS) under denaturing conditions. (Wagner et al., 2020). The CE-SDS method has proven to be an important method for assessing heterogeneity in size, purity, and stability of products. Reports from the early 1990s support the use of this method for mAb analysis. A 2008 publication from Rustandi et al. (2008) showed that CE-SDS is capable of assessing a wide range of parameters such as quantification of non-glycosylated heavy chains (NGHCs) or antibody stability in relation to conditions such as temperature, light exposure, buffer pH, or formulation.

CHAPTER 2: Investigating Factors that Influence Virus Filtering Ability of IgG

2.1 Introduction:

There is an inherent risk of viral contamination in therapeutic products derived from biological sources. It is known that mammalian cell cultures used in the manufacture of recombinant biotherapeutics endogenously express retrovirus-like particles and are susceptible to adventitious viral infections (Barone et al., 2020; Leisi et al., 2022). Blood-borne viruses may be present in plasma donations, which serve as raw material for the manufacture of plasma-derived medicines, such as polyclonal human immunoglobulin G (IgG). A multilayered strategy is employed by manufacturers to mitigate the risk of viral contamination by rigorous monitoring of raw materials and testing of sources, while incorporating effective virus clearance steps to eliminate potentially present viruses during downstream processing (ICH., 1998). Virus filtration is an effective and robust method to remove any viral contaminants introduced into the manufacturing process based on size-exclusion mechanism using a porous membrane operated in the normal filtration mode (Namila et al., 2019). In order to approve a new therapeutic, regulatory agency such as the US Food and Drug Administration (FDA) require validation of adequate virus clearance (FDA, 1997). The purification train is therefore modified to include unit operations for high virus clearance levels (Han et al., 2002). The virus filtration process uses membranes with large pores to retain contaminating viruses while recovering virus-free products. There is a much higher level of performance criteria for virus filters compared to conventional ultrafiltration operations (Billups et al., 2021). The membrane-based separation method is preferable since it is simple to operate and causes little damage to proteins. Consequently, virus filters are single-use devices because disposable systems are cost-effective and user-friendly, without the need for cleaning and further validation (Namila, 2020). The use of polymeric

membranes with nominal pore sizes of 19–20 nm as parvovirus-grade filters allows the selective separation of therapeutic proteins, such as IgGs with a hydrodynamic diameter of 10–12 nm, from parvoviruses with a 27–29 nm outer capsid diameter (Leisi et al., 2022; Roth et al., 2020).

In the downstream manufacturing of biotherapeutics, macromolecules can self-associate, aggregate, or interact with surfaces, including polymeric filter materials, causing membrane fouling. Fouling of the membrane is a critical challenge in virus filtration that reduces product throughput and compromises virus removal effectiveness (Bolton et al., 2005; David et al., 2019). There is a common understanding that flow decay occurs in protein filtration because of irreversible fouling caused by protein aggregates that are formed before or during filtration (Kelly et al., 1993; Kosiol et al., 2019; Rayfield et al., 2015). The presence of trace quantities of protein species with self-association propensity in the feedstream can serve as nucleation sites for bulk protein deposition in the sieving layer of the membrane (Fallahianbijan et al., 2021; Kanani et al., 2008; Kelly & Zydney, 1994). It has been suggested that prefilters can considerably improve the throughput of IgG feedstream in virus filtration by eliminating hydrophobic, self-associating protein species, such as oxidized and degraded IgG forms (Bolton et al., 2006, 2010; Stanevich et al., 2021).

Several factors affect intra- and intermolecular interactions between proteins in the feedstream and membrane, including their isoelectric point (pI), the pH of the solution, and the conductivity. Accordingly, fouling is significantly affected by filtration conditions, therapeutic proteins, and filter membranes (Namila et al., 2019; Rayfield et al., 2015). Therefore, it is crucial that these factors are studied and controlled carefully to reduce membrane fouling and maximize product throughput. The purpose of this study is to investigate the effect of buffer type, salt content, protein molecules, and filter properties on the fouling of virus filters.

2.2 Material and Methods

2.2.1 Materials

The buffer preparation was performed using the following reagents: sodium chloride (biotechnology grade) from VWR Life science (Radnor, PA), sodium phosphate monobasic monohydrate (ACS reagent, ≥98%) and anhydrous sodium phosphate dibasic from Millipore Sigma (Reagent Plus®, ≥99.0%) (St. Louis, MO), tris base (biotechnology grade) from G-BioSciences (St. Louis, MO), Sodium citrate dihydrate (molecular biology grade) was obtained from EMD Millipore (Billerica, MA). RNase was from Bio Basic. Insulin was from MP Biomedicals.

SDS-MW gel buffer, acidic and basic wash solutions, MW ladder, 10 kDa internal standard, and Tris/SDS sample buffer (pH 9.0) were purchased as a kit from Sciex Separations (Framingham, MA). Precision protein plus MW standard was sourced from Bio-Rad laboratories (Hercules, CA). 2-mercaptoethanol was provided from EMD Millipore (Billerica, MA). Coomassie brilliant blue R-250 was purchased from Bio-Rad Lab-oratories (Hercules, CA). Iodoacetamide (IAM) (≥98 %) was purchased from VWR Life science (Radnor, PA).

Nalgene™ rapid-flow™ bottle top filters (0.2 μm and 0.1 μm) were sourced from ThermoFisher Scientific (Waltham, MA). Other prefilters used in this study were Viresolve pre-filter (VPF) (5 cm^2) provided by EMD Millipore (Billerica, MA), Planova 75N (10 cm^2) provided by Asahi Kasei Medical (Tokyo, Japan). The selected virus filters were Viresolve® Pro filter (3.1 cm^2) provided by EMD Millipore (Billerica, MA), and Planova BioEX (3cm^2) provided by Asahi Kasei Medical (Tokyo, Japan).

2.2.2 Protein Feed Solution Preparation and Characterization

A human plasma IgG (Human Gamma Globulin 95% purity) used in this study was provided by NOVA (Biologics, INC). IgG solution was prepared fresh for each experiment by dissolving the appropriate amount of protein powder in 50 mM sodium phosphate buffer without and with 200 mM NaCl (pH 7.0) at room temperature to reach a concentration of 200 g/L. The solution was then serially diluted using the same buffer to a concentration of 160, 120, 80,40,20,10 and 5 g/L.

Measurement of protein concentration and turbidity was performed by measuring the absorption at 280 nm using Genesys 10 UV scanning system (Waltham, MA) with VWR quartz spectrophotometer cell (path length 1 cm) (West Chester, PA).

2.2.3 Protein Filtration

Prior to filtration, protein solutions were first prefiltered with 0.2 μm or 0.1μm bottle top filters to remove any large aggregates or hydrophobic foulants. VPF prefilter and VPro virus filter were initially wetted with Deionized water filtered with 0.2 μm bottle-top filter into the Planova pressure reservoir (Asahi Kasei, Japan) by closing the outlet and opening the vent under 1-2 psi with the pressure controlled by Ashcroft pressure gauge (Part number: EW-68334-15; 0-100 psi, resolution 0.1, accuracy ± 0.5 full-scale). After that, they were flushed with 100 L/m² of DI water, followed by 100 L/m² of equilibration buffer to ensure complete wetting and to remove any air bubbles trapped in the system. Industrial grade nitrogen at 10.0 psi was used to pressurize the feed reservoir. Prefiltered protein solution was gently poured down the vessel wall. Filtration was conducted by closing the feed side vent, sending the gas to the filter, and filtering at constant pressure of 30 psi.

The Planova 75N prefilter and BioEX virus filter were tested for pre-use integrity using visual leakage testing (VLT) by air-pressurizing the system with industrial-grade nitrogen at 14 psi, placing the filter horizontally, and watching it for at least 20 seconds. If the filter is free of continuous bubbling during VLT, then priming, water flush, buffer flush and virus filtration steps were performed following the same procedure as for VPF and VPro membranes except that the feed reservoir was pressurized at 11.2 psi with 75N and 45 psi with BioEx.

A Mettler Toledo scale (Columbus, OH) was connected to BalanceLink software to record the cumulative weight of the filtrate every minute. The data collected was used to calculate the filtrate flux. Protein recovery was determined by measuring the absorbance at 280 nm with a spectrophotometer to determine the protein concentration of the feed and each filtrate fraction.

2.2.4 Size Exclusion Chromatography

The size exclusion chromatography (SEC) technique with a TSK Gel 3000 SWXL column (30 cm L 7.8 mm ID., Tosoh Bioscience, LLC) was performed on a high-performance liquid chromatography instrument (Agilent 1260 Infinity Quaternary LC) manufactured by Agilent Technologies (Santa Clara, CA) using a TSK Gel 3000 SWXL column (30 cm L 7.8 mm ID., Tosoh Bioscience, LLC) consisting of a quaternary pump with degasser, an autosampler with a cooling unit, a column oven, and a DAD detector. Prior to analysis, the samples were filtered through a 0.2 μm polyethersulfone (PES) syringe filter. The separation was carried out at a flow rate of 1.0 mL/min with a sample injection volume of 10 μL. The mobile phase was 50 mM sodium phosphate without and with 200 mM NaCl at pH 7.0 filtered with a 0.2 μm bottle top filter. UV absorbance peaks were detected at 280 and 220 nm to determine the relative amounts of monomer and product variants.

2.2.5 Dynamic Light Scattering and Diffusion Interaction Parameter

Dynamic light scattering (DLS), a method for the investigation of the hydrodynamic radius and diffusion coefficient of the IgG was conducted with a Delsa™ Nano particle size analyzer (Beckman Coulter, Brea, CA). Protein solutions were filtered with a 0.2 μm polyethersulfone (PES) syringe filter before transferring a 1 mL aliquot into a disposable polystyrene cuvette with a 1 cm pathlength (BrandTech, Essex, CT). Three repeats with different aliquots were carried out for each sample and 300 acquisitions in each repeat were used to record the DLS data. The software was used to analyze the collected data, which resulted in a mean hydrodynamic dynamic diameter and a diffusion coefficient for IgG at each concentration in each solution condition. The diffusion coefficient and hydrodynamic radius of a molecule can be calculated using the DLS intensity data using Equation 2.1 listed in chapter 2.

2.2.6 Sodium Dodecyl Sulfate (SDS) Polyacrylamide Gel Electrophoresis (PAGE) analysis

SDS-PAGE analysis of IgG was carried out under reducing and non-reducing conditions in pre-cast polyacrylamide gels to characterize molecular-size distributions. Samples were first diluted to 2 mg/mL in Laemmli sample buffer, with or without adding 5% (v/v) 2ME (2 mercaptoethanol). After incubating for 10 min at 95 ◦C in order to denature the proteins and, for samples with 2ME, to reduce disulfide bonds. The samples and molecular weight standards (Mark 12) were loaded onto the gels. Electrophoresis was carried out at a constant voltage of 200 V with a 1× Tris-glycine–SDS running buffer. Following electrophoresis, gels were stained overnight (18 ± 2 h) using Coomassie blue and de-stained with destaining solution (10% acetic acid, 40% methanol, and 50% water).

2.2.7 Capillary Electrophoresis –SDS Molecular weight (CE-SDS MW) analysis

IgG were analyzed using the capillary electrophoresis instrument (PA 800 plus) to identify MW variants, charge variants, glycovariants, and impurities. The instrument parameters included a 50 μM ID and a 30 cm total length of bare fused silica capillary which was filled with the SDS-MW gel-buffer system.

Samples were diluted with CE-SDS Sample Buffer to a final concentration of 1 mg/mL. Then, 2 μL of Internal Standard was added to each sample. 5 μL of a 250 mM stock solution of the alkylating agent IAM was added to each sample to block disulfide scrambling or exchange. Samples were denatured at 70◦C for 3 min and mixed by vortex, cooled on ice for 5 min and mixed by vortex. The samples were then transferred to 96-well plates and centrifuged at 1000 x g for 10 min. Up to 72 samples can be loaded at once. Characterization takes place sequentially based on the programmed software instructions. The data acquisition and processing were carried out using the 32Karat software package.

2.2.8 Relative Hydrophobicity Analysis (RH)

Relative surface hydrophobicity (RH) analysis of IgG solution was conducted on Tosoh TSK Phenyl 5PW column (Tosoh Biosciences, LLC) connected to FPLC ÄKTA Pure (GE Healthcare Bio-Sciences Corp., Boston, MA, USA) at 0.75 mL/min utilizing a linear gradient from 100% Buffer A to 100% Buffer B. The initial linear gradient was run from 100% Buffer A (0.5 M sodium citrate in 10 mM tris, pH 8.0) to 100% Buffer B (10 mM tris, pH 8.0). As a system suitability test, two protein standards were used: ribonuclease A (RNAse A) (has the smallest RH), and insulin (has the largest RH); all the proteins had the concentration of 0.1% in buffer A solution. The column was first pre-saturated with buffer A for 30 min before running the program method. For the program method, equilibration was carried out for 20 min (buffer

A), sample loading (150 μL), and gradient solvent (0 to 100% buffer B) for 25 min followed by 100% buffer B for 10 min. A relative hydrophobicity value was calculated by first dividing the retention times of the solutes in the gradient by the salt concentrations. This hydrophobicity value of this protein was then normalized according to reference protein standards of RNase and insulin as follows:

$$\boldsymbol{X_{normalized}} = \frac{X - X_{min}}{X_{max} - X_{min}} = \frac{X_{sample} - X_{RNAse}}{X_{insulin} - X_{RNAse}} \quad \text{(Equation 2.1)}$$

Based on this calculation, the solutes were ranked according to their relative hydrophobicity on a 0–1 scale, with zero being the lowest and one being the highest.

2.3 Results and Discussion

2.3.1 Virus Filtration and Prefiltration Results

2.3.1.1 Viresolve® Pro Filtration with Prefiltration

The Viresolve® Pro virus filter was used in-line with VPF pre-filter to filter different concentrations of IgG in 50 mM sodium phosphate buffer with 200 mM NaCl at pH 7.0. The IgG solution was filtered with a 0.2 μm sterile filter. The filtration was performed at a constant pressure of 210 kPa (30 psi), as recommended by the filter manufacturer. The results are plotted as normalized fluxes in relation to volumetric throughput. Figure 3.1. below shows the flux decay associated with filtration of IgG through VPro virus filter. Significant fouling of the membrane and flux decay was observed at the high concentrations of IgG (9-3 g/L) and the prefiltration with 0.2 μm bottle top filter and the VPF prefilter were ineffective. The high degree of fouling seen with the 9 g/L IgG is due to the high concentration of aggregate in this polyclonal IgG. IgG solution at 2 g/L showed the much lower rate of fouling, with flux decreasing by 10%

after filtration of approximately 200 L/m². Table 3.1 shows mass balance and protein recovery for VPro filtration fractions that were performed using UV absorbance measurements at 280 nm.

It can be concluded that within the variability of the testing data this in-line filter did not provide much benefit in improving the filtrate flux at high concentrations of IgG solution, and virus filter fouling is strongly affected by the concentration of the feed solution. In addition, the fouling species, based on the high purity of the feed, are probably product aggregates and thereby pass through the pre-filter to the virus filter.

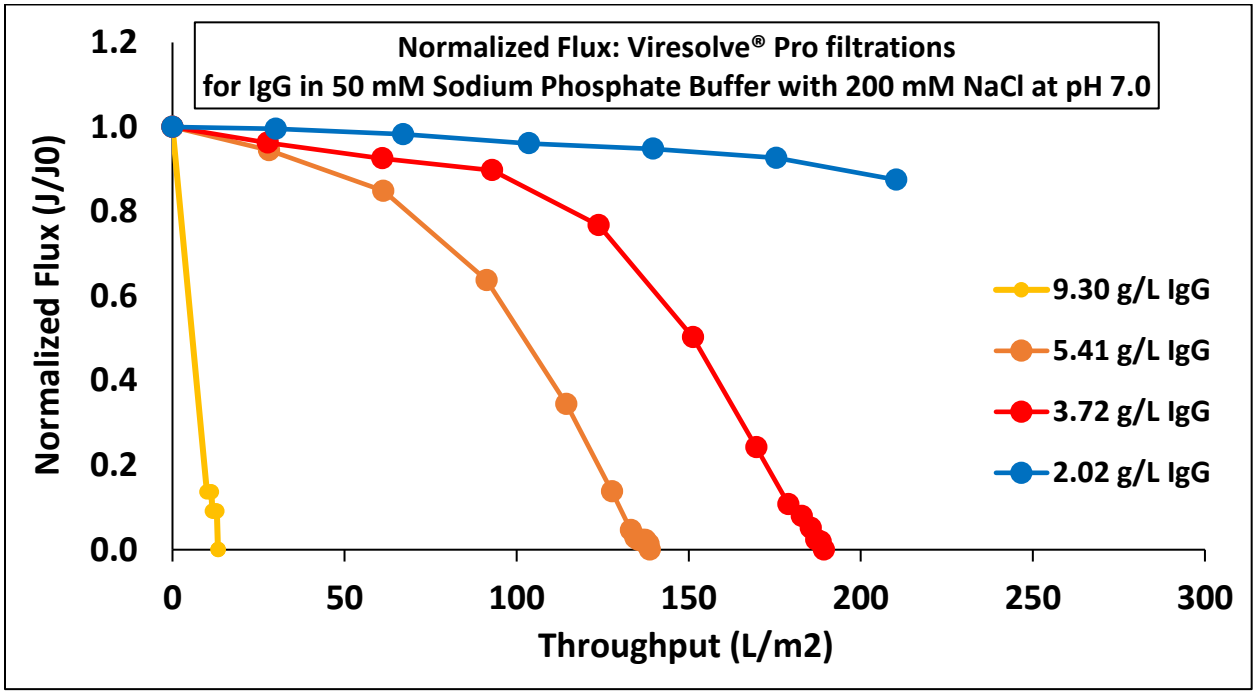

Figure 2.1 Virus filtration experiments with Viresolve® Pro after pre-filtration with VPF were performed for different concentrations of IgG in 50 mM sodium phosphate buffer with 200 mM NaCl at pH 7.0.

Table 2.1 Virus filtration experiments with Viresolve® Pro after pre-filtration VPro filtration fractions in 50 mM sodium phosphate buffer with 200 mM NaCl at pH 7.0.

VPro Filtration of IgG in 50 mM sodium phosphate with 200 mM NaCl, pH7.0				
Tube 1	**Dilution factor**	**Abs @ 280 nm**	**Concentration (mg/mL)**	**Mass (mg)**
Feed	**x100**	**0.11**	**9.3**	**40.92**
VPro filtrate	**x50**	**0.13**	**5.5**	**24.2**
VPro buffer chase pH7	**x10**	**0.1**	**0.84**	**1.68**
VPro buffer elute pH4	**no dil.**	**0.07**	**0.05**	**0.15**
VPro buffer elute pH9	**no dil.**	**0.002**	**0.001**	**0.003**
IgG recovery	**63.61%**			
Tube 2	**Dilution factor**	**Abs @ 280 nm**	**Concentration (mg/mL)**	**Mass (mg)**
Feed	**x40**	**0.16**	**5.41**	**233.71**
VPro filtrate	**x10**	**0.53**	**4.48**	**193.53**
VPro buffer chase pH7	**x10**	**0.50**	**4.22**	**8.44**
IgG recovery	**86.41%**			
Tube 3	**Dilution factor**	**Abs @ 280 nm**	**Concentration (mg/mL)**	**Mass (mg)**
Feed	**x10**	**0.44**	**3.72**	**219.48**
VPro filtrate	**x5**	**0.77**	**3.25**	**191.75**
VPro buffer chase pH7	**x5**	**0.71**	**3**	**2.1**
IgG recovery	**88.32%**			
Tube 4	**Dilution factor**	**Abs @ 280 nm**	**Concentration (mg/mL)**	**Mass (mg)**
Feed	**x10**	**0.24**	**2.02**	**160.18**
VPro filtrate	**x5**	**0.42**	**1.77**	**140.36**
VPro buffer chase pH7	**No**	**0.07**	**0.06**	**0.89**
VPro buffer elute pH4	**No**	**0.07**	**0.06**	**0.69**
VPro buffer elute pH9	**No**	**0.07**	**0.06**	**0.7**
IgG recovery	**89.04%**			

2.3.1.2 BioEx Filtration with and without Prefiltration

Planova 75-N was used as prefilter with Planova BioEX virus filter to filter 10 g/L IgG. The bottle-top 0.1-μm size exclusion-based sterile filter was also used as prefilter. Figure 3.2 shows that 0.1 μm and 75N prefilters do not improve BioEX filter flux and are ineffective in

foulant capture. Significant flux decay was observed, and the overall throughput was less than 25 L/m² of feed IgG at 10 g/L.

The Planova BioEX virus filter was also used to filter 10 g/L IgG in two runs. Figure 3.3 below shows the flux decay associated with IgG filtration through the BioEX virus filter. In run 2, the permeate from run 1 BioEX filtration was introduced into a second BioEX filter. The second run shows less fouling and significant flux improvement because some of the fouling species were captured in the first run. The application of post-filtration buffer flush with different conditions results in higher flux recovery in the second run than the first run. IgG in the first run exhibited a continuous drop in filter flux falling to 0 %. The following buffer flush with pH7, pH4 and pH9 reached flux values in the range of ~80, 70 and 20% respectively, while in the second run IgG exhibited less decrease in flux to value of approximately 60%. However, the buffer flush following the IgG filtration results in the flux recovery on the fouled virus filter in all conditions. This indicates that filter fouling is reversible since aggregated biomolecules are resolubilized and released into filterable molecules by desorption and resolubilization. This observation was also reported by Bieberbach et al. (2019) virus filter flux decay can be caused by two types of fouling species: irreversible aggregates and reversible aggregates. The fouling caused by reversible aggregates results in concentration-dependent initial flux decay. Buffer chases can mitigate flux reductions caused by concentration-dependent reversible protein oligomer formation by diluting the feed. This applies only when the virus titer in the feed solution is high. The mass balance for IgG fractions of run 1 and run 2 fractions is shown in Table 3.2 below.

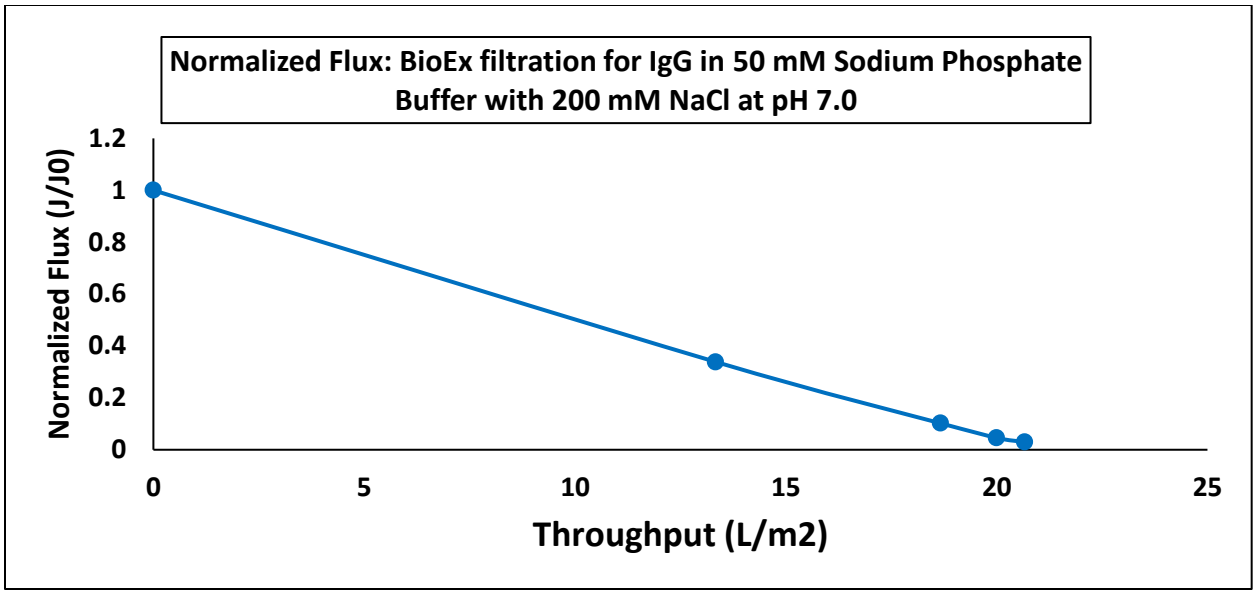

Figure 2.2 Virus filtration experiment with BioEx filter after pre-filtration with Planova 75N were performed for 10 g/L IgG in 50 mM sodium phosphate buffer with 200 mM NaCl at pH 7.0.

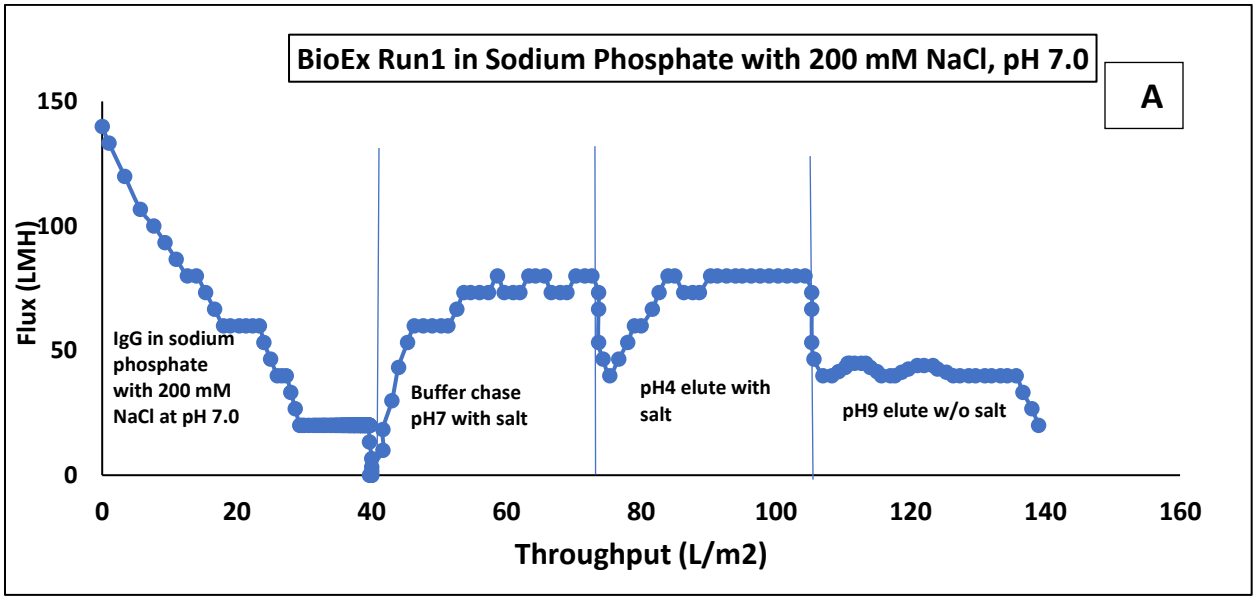

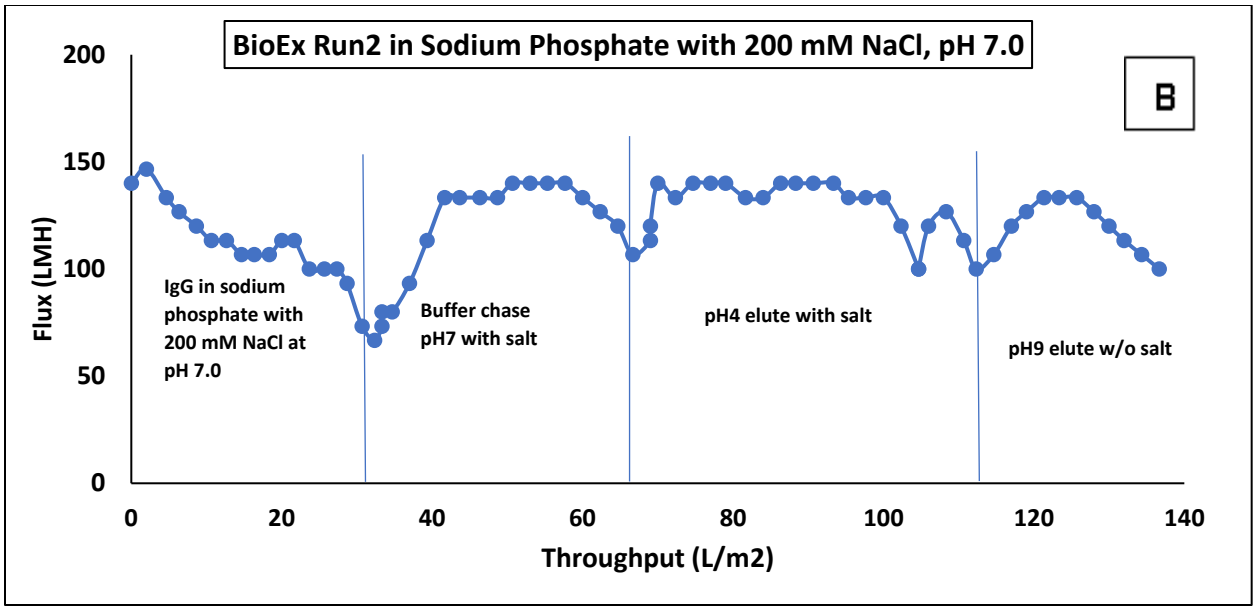

Figure 2.3 Virus filtration experiment with BioEx **(A)** run1 **(B)** run2 were performed for 10 g/L IgG in 50 mM sodium phosphate buffer with 200 mM NaCl at pH 7.0.

Table 2.2 Mass Balance for IgG BioEx filtration fractions in 50 mM sodium phosphate buffer with 200 mM NaCl at pH 7.0.

BioEx filtration of IgG run1				
Tube	Dilution factor	Abs @ 280 nm	Concentration (mg/mL)	Mass (mg)
feed	x100	0.13	11.09	133.08
BioEx filtrate run1	x10	0.40	3.39	40.68
Buffer chase pH7	x10	0.30	2.54	25.40
Buffer elute pH4	No dil.	0.11	0.08	0.76
Buffer elute pH9	No dil.	0.10	0.08	0.80
IgG recovery	50.82%			
BioEx filtration of IgG run2				
Tube	Dilution factor	Abs @ 280 nm	Concentration (mg/mL)	Mass (mg)
feed filtrate from BioEx run1	x10	0.40	3.39	33.90
BioEx filtrate run2	x10	0.21	1.69	16.90
Buffer chase pH7	No dil.	0.20	0.17	1.81
Buffer elute pH4	No dil.	0.22	0.17	1.70
Buffer elute pH9	No dil.	0.14	0.11	1.10
IgG recovery	63.45%			

2.3.2 Characterization of IgG

2.3.2.1 Size Exclusion Chromatography (SEC) Analysis of IgG

Different concentrations of IgG were analyzed using SEC in pH 7 sodium phosphate buffer without and with 200 mM NaCl to investigate the effects of buffer and pH condition as well as product titer on protein aggregation and ultimately on virus filtration to select an appropriate buffer condition. The SEC chromatograms are shown in Figure 3.4 The percentages of monomeric and dimeric IgG were calculated and tabulated in Table 3.3 The range of dimeric percentage varies from less than 1% to ~ 6% for product titer of 40 g/L or below. However, it increases to about 10% when product titer is 80 g/L or above. The presence of trimer is detected (1-2%) at high product titers. Thus, aggregate concentration increases slightly as the IgG concentration increases. In addition, there is some slight differences in the presence and absence of 200 mM NaCl. The aggregate concentrations in the presence of 200 mM are slightly lower than the corresponding solutions without NaCl except at 5 g/L condition. It is known that protein conformation, stability and solubility are affected by the presence of salt as reported by Rosenberg (2010) . Kunz et al. (2004) showed that the presence and the absence of the slat can affect the solubility of protein molecules.

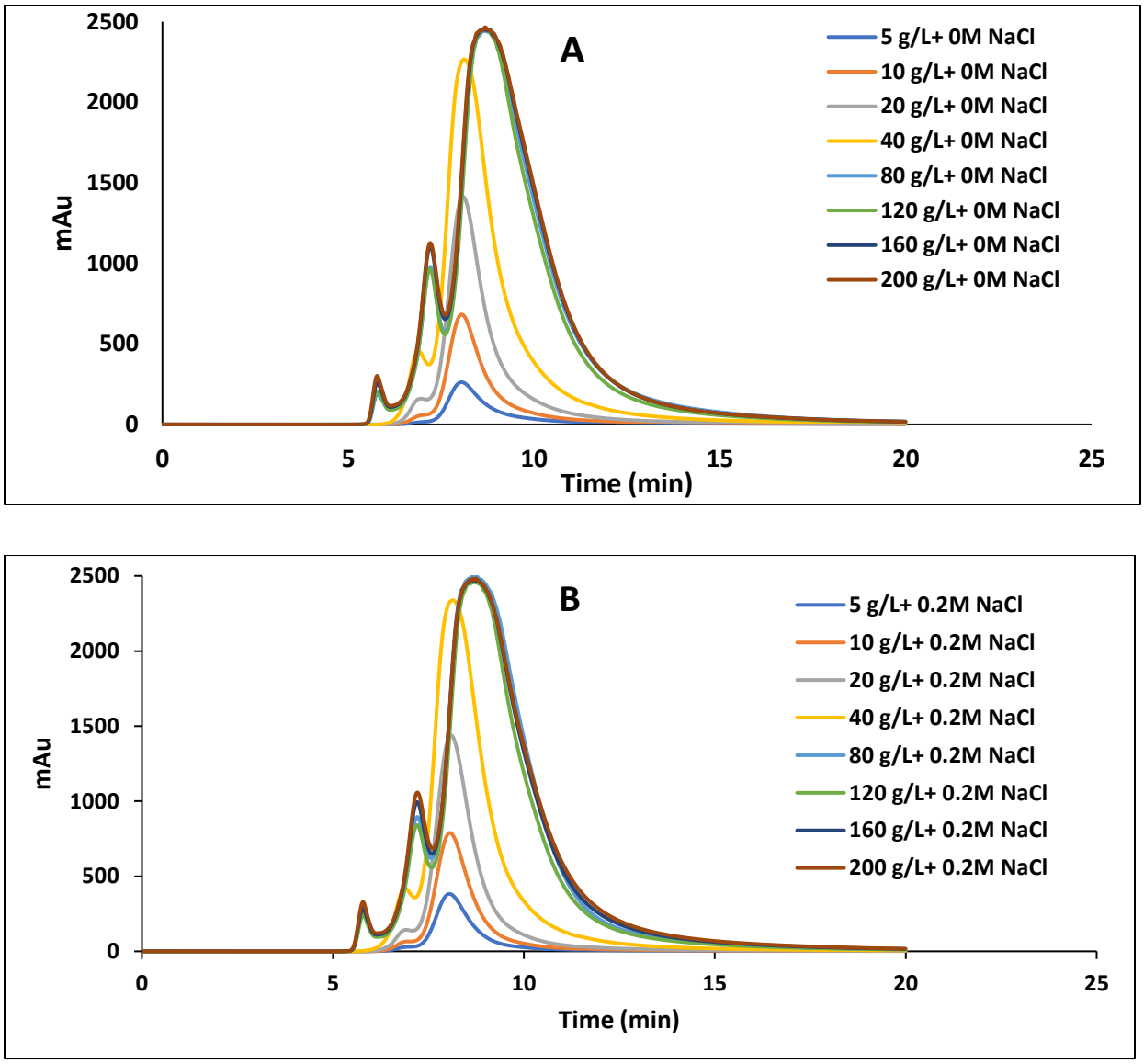

Figure 2.4 Size -Exclusion Chromatogram of IgG at different concentrations in 50 mM sodium phosphate buffer **(A)** without salt and **(B)** with 200 mM NaCl at pH 7.0.

Table 2.3 The percentage of monomer and dimer present at different concentrations in 50 mM sodium phosphate buffer **(A)** without salt and **(B)** with 200 mM NaCl at pH 7.0.

A.

Buffer	**50 mM Phosphate Buffer at pH 7.0 0 mM NaCl**							
IgG (g/L)	5	10	20	40	80	120	160	200
Trimer %	-----	-----	-----	-----	0.91	1.12	1.24	1.34
Dimer %	1.62	3.34	3.88	6.27	10.13	10.48	10.94	11.15
Monomer %	98.37	96.56	96.12	93.73	88.95	88.39	87.80	87.49

B.

Buffer	**50 mM Phosphate Buffer at pH 7.0 200 mM NaCl**							
IgG (g/L)	5	10	20	40	80	120	160	200
Trimer %	-----	-----	-----	-----	1.40	1.50	1.47	1.71
Dimer %	2.90	2.89	3.82	5.86	9.43	9.94	10.52	11.06
Monomer %	97.10	97.11	96.18	94.14	89.16	88.55	88.0	87.22

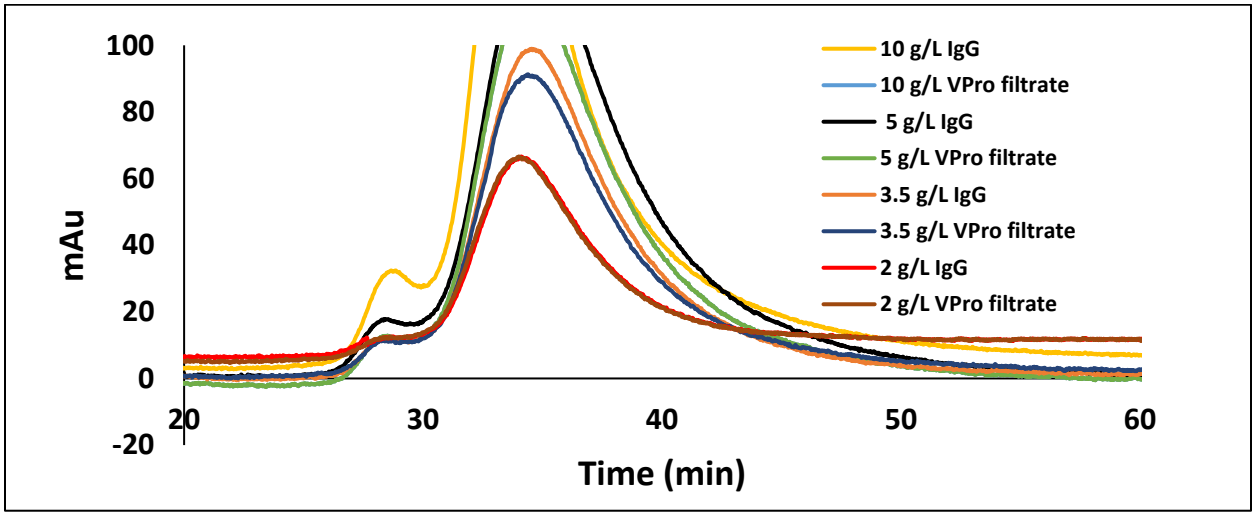

Figure 2.5 Size -Exclusion Chromatogram of IgG VPro filtration fractions in 50 mM sodium phosphate buffer with 200 mM NaCl at pH 7.0.

Table 2.4 The percentage of monomer and dimer present of IgG VPro filtration fractions in 50 mM sodium phosphate buffer with 200 mM NaCl at pH 7.0.

IgG Concentration	Area %	Feed	VPro Filtrate
10 g/L	Dimer	3.40	2.55
	Monomer	96.60	97.45
5 g/L	Dimer	2.03	1.96
	Monomer	97.96	98.03
3.5 g/L	Dimer	1.83	1.44
	Monomer	98.16	98.55
2 g/L	Dimer	1.35	1.30
	Monomer	98.64	98.69

SEC characterization was also performed for VPro filtration fractions of IgG in pH 7 sodium phosphate buffer (200 mM NaCl) with prefiltration. Table 3.5 shows the percentages of monomeric and dimeric species of IgG based on SEC chromatography that are shown in Figure 3.4; the dimeric concentration increases slightly as the IgG concentration increases. In the concentrations 2 and 3.5 g/L, protein aggregation is relatively low, however, when the IgG concentration increases to 5 and 10 g/L, the percentage of aggregates increases to ~2 and 3% respectively. The aggregate concentrations in the feed are slightly higher than the filtrate and a higher dimer concentration is observed at higher IgG concentration. Thus, the difference in flux with decreasing IgG concentration can be explained by the SEC measurements, suggesting that this phenomenon is caused by pore-plugging with dimeric species. However, the pre-filters were able to mitigate initial and continual flux decline at the lowest concentration of IgG. Brown et al. (2010) report that dimeric and multimeric species clog virus removal membrane pores, thereby decreasing the performance of filters. Kelly et al (1993). also found that virus filter fouling was

highly correlated with the composition of dimeric and multimeric species by using SEC to characterize BSA solution.

2.3.2.2 Dynamic Light Scattering (Particle Size Analysis) of IgG

Dynamic Light Scattering (DLS) was used to investigate the hydrodynamic diameters of the IgG protein at different concentrations in pH 7 sodium phosphate buffer without and with 200 mM NaCl. Shown in Figure 3.6 are the intensity vs protein particle size measurements for IgG solution in the presence and absence of salt. Table 3.5 exhibits the calculated average hydrodynamics diameters for the different buffer and protein concentration conditions. The protein is slightly more compact in the presence of 200 mM NaCl than without salt. In addition, the hydrodynamics diameter increases as the increase of protein concentration indicating a stronger tendency to associate in agreement with the SEC studies.

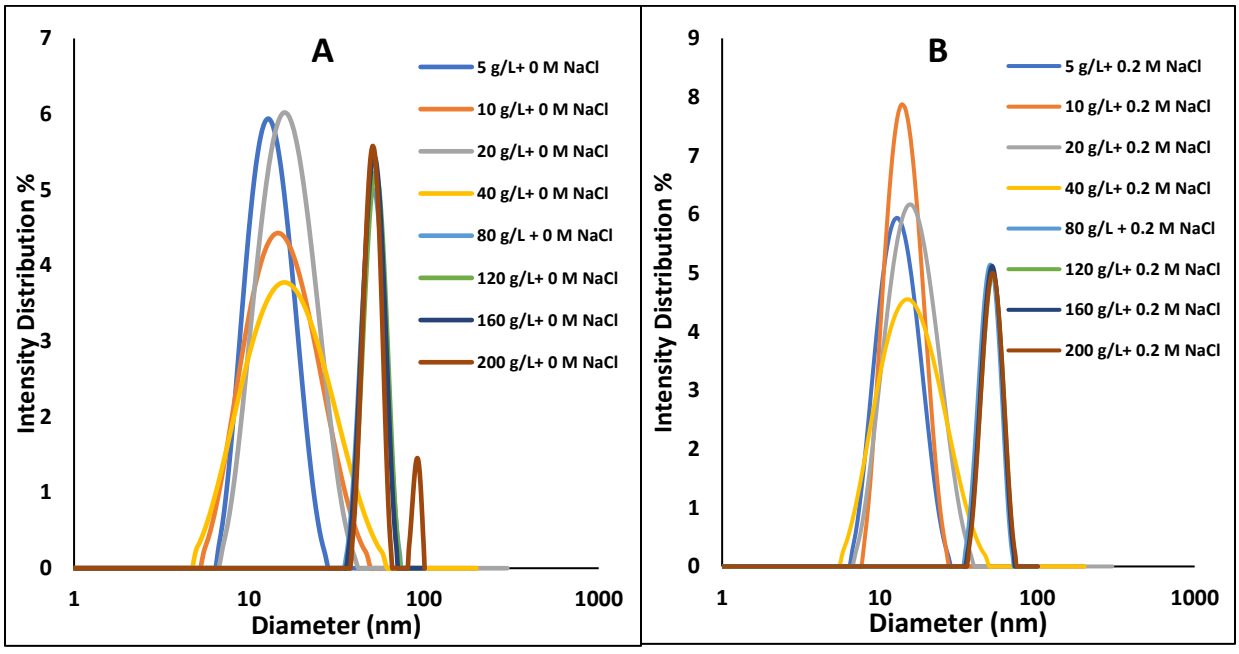

Figure 2.6 Size distribution of IgG in 50 mM phosphate buffer **(A)** without salt, **(B)** with 200 mM NaCl at pH 7.0.

Table 2.5 The average hydrodynamic diameter (nm) of IgG in 50 mM phosphate buffer without salt and with 200 mM NaCl at pH 7.0.

Buffer Condition	**Hydrodynamic Diameter of IgG (nm)**			
50 mM Sodium Phosphate, pH 7.0	**0 Mm NaCl**			**200 Mm NaCl**
IgG concentration (g/L)	**5**	**13.7 ± 4.0**		**13.1 ± 2.2**
	10	**16.9 ± 7.7**		**14.6 ± 3.7**
	20	**17.3 ± 6.1**		**16.9 ± 5.9**
	40	**18.7 ± 9.9**		**17.1 ± 7.6**
	80	**24.2 ± 11.5**		**21.7 ± 9.7**
	120	**25.2 ± 11.1**		**24.4 ± 11.3**
	160	**26.4 ± 11.6**		**26.5 ± 12.4**
	200	**Peak 1**	**23.6 ± 8.1**	**28.61± 13.8**
		Peak 2	**282.3 ± 75.0**	

Based on the hydrodynamic radius from DLS measurement, diffusion coefficient can be measured for the IgG molecules at each specific solution condition. Figure 3.7 shows the calculated diffusion coefficient as a function of the IgG concentration in the 50 mM phosphate buffer with and without 200 mM NaCl. The two buffers modulate the protein interaction slightly differently. In both buffers, the protein tends to have attractive interactions. The magnitudes of the interaction seen from the slopes of the two plots are somewhat different. From the data points so far, the k_D value for the IgG in 0 mM NaCl is -49.50 mL/g. The corresponding value in 200

mM NaCl is -34.75 mL/g. These results indicate that IgG molecules in the 50 mM phosphate buffer without salt tend to have a stronger tendency to aggregate compared to the condition with 200 mM NaCl. The presence of salt stabilizes the protein at low product concentrations (<50 g/L). However, it causes aggregation at high product concentrations (160-200 g/L). This can also be observed from the hydrodynamic diameter of the protein in the two conditions. The larger hydrodynamics diameter of the protein without salt indicates that the interaction of the molecules is stronger than the corresponding buffer with 200 mM NaCl at the same IgG concentration.

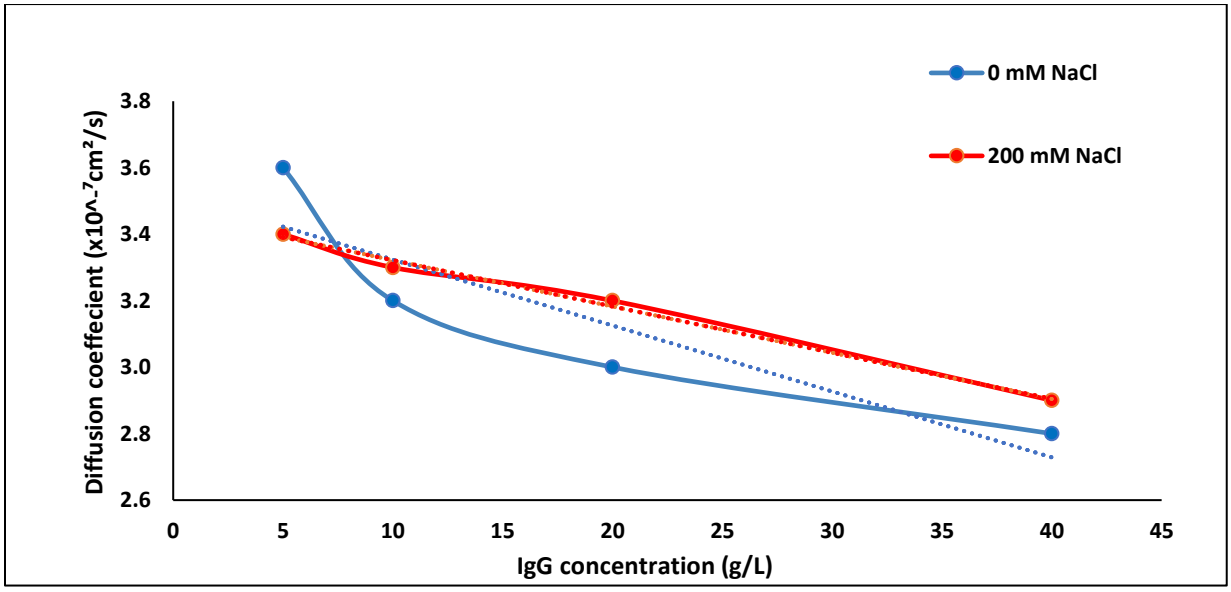

Figure 2.7 The diffusion coefficient of the IgG measured by DLS at different concentrations in 50 mM phosphate buffer without and with 200 mM NaCl at pH 7.0.

k_D **of IgG in 50 mM sodium phosphate buffer at pH 7.0**	
0 mM NaCl	**200 mM NaCl**
-49.50 mL/g	**-34.75 mL/g**

Table 2.6 The calculated diffusion interaction parameter, k_D, in the two solution conditions.

2.3.2.3 Capillary Electrophoresis CE-SDS Analysis of IgG

IgG samples were characterized by CE-SDS on the PA 800 plus to detect the fine fragmentation of IgG as shown on the electropherograms in Figure 3.8. Samples were analyzed under non-reducing and alkylating conditions to determine the fragmentation species of IgG in their original state. It is in this context that fragmentation species consist primarily of native antibody subunits represented by light chain (L, 25 kDa), heavy chain (H, 50 kDa), heavy-light (HL, 75 kDa), heavy-heavy (H2, 100 kDa) and heavy-heavy-light (H2L, 125 kDa), which are separated from the intact mAb (H2L2, 150 kDa) and identified by their relative migration times (Wagner et al., 2020).

The CE-SDS electropherogram of IgG exhibited a typical heavy-heavy-light chain peak that increased as IgG concentration increased. A small peak of fragmented heavy-heavy chain was also observed at 100 kDa. Indicating that in the case of non-reduced CE-SDS, denaturation affects the stability of IgG and increases fragmentation levels.

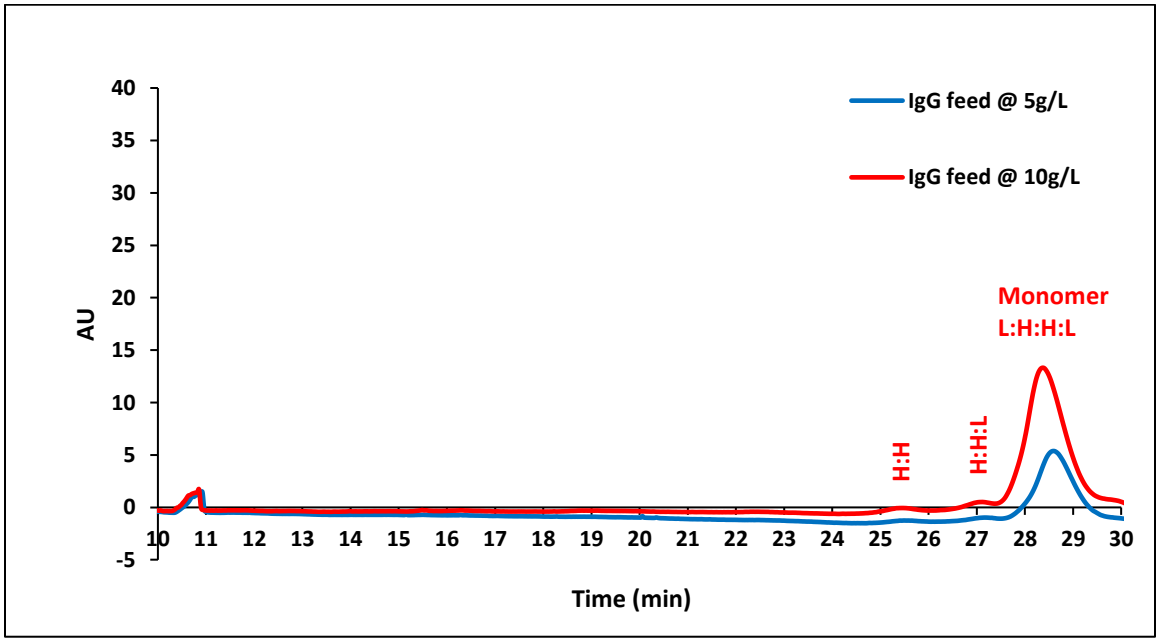

Figure 2.8 CE-SDS Chromatogram of IgG in 50 mM sodium phosphate buffer at pH 7.0.

2.3.2.4 SDS-PAGE analysis for IgG

Analysis of IgG BioEx filtration fractions was conducted by gel electrophoresis as a second method to characterize the molecular-size distribution. An image of the gel is shown in Figures 3.9a and b. SDS-PAGE of IgG was carried out in non-reducing as well as reducing conditions on 14% separating gel and 4% stacking gel with a voltage of 200v. The IgG monomers in the feed and filtrate do not break down into heavy (50 kDa) and light (25 kDa) chains in the non-reducing condition. Each shows a strong band at about 250 kDa. Despite IgG's nominal molecular mass of about 150 kDa, it may run abnormally in this gel due to its unreduced nature and to glycosylation's effects on protein mobility. Additionally, each sample shows a high-molecular-mass band corresponding to IgG aggregates, while the reducing condition causes IgG samples to be reduced into its component parts: heavy (50 kDa) and light (25 kDa) chains. In both the unreduced and reduced conditions, the feed and filtrate samples show the same pattern of bands. The non-reducing condition gave better results for SDS-PAGE analysis because it detects proteins with a higher molecular weight (Bolton et al., 2006).

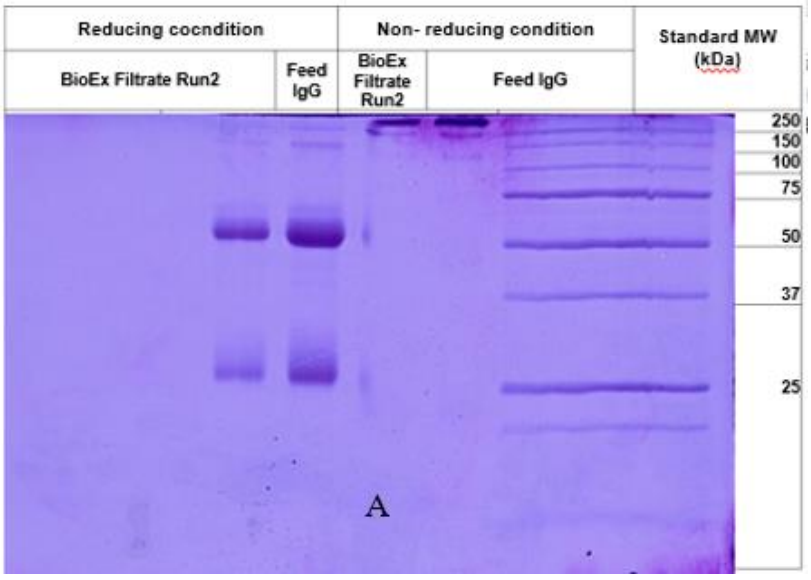

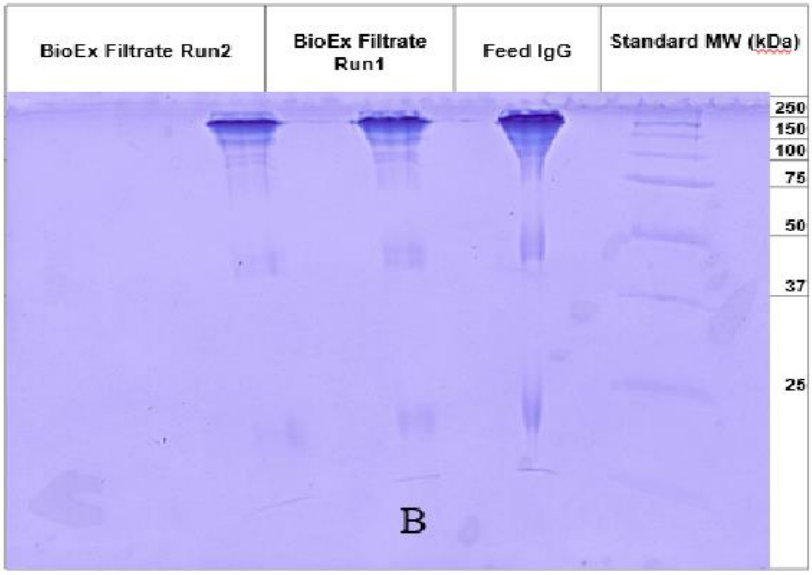

Figure 2.9 SDS PAGE of IgG BioEX Filtration Fractions without Prefiltration **(A)** reducing and non-reducing conditions. **(B)** Non- reducing condition.

2.3.2.5 Relative Hydrophobicity Scale of IgG

Relative surface hydrophobicity assay (RH) of IgG was performed using Tosoh TSK Phenyl 5PW column (Tosoh Biosciences, LLC) following the reference method; however, the gradient solvent used was slightly modified to meet the elution sodium citrate concentration gradient of 0.5 M to nearly 0 M within the running time of 35 minutes. In Figure 3.10a the result shows that IgG elution corresponded with the visible UV peak (around 13.7 minutes into the gradient). Figure 3.10b shows the RH values for IgG sample and protein standards. Protein standards and IgG is plotted according to the salt concentration at which they were determined to elute from the column. A sample was also plotted according to its RH as determined through comparison to the protein standards. The citrate concentration at this point was about 200 mM. comparing this value to two model protein standards, IgG score RH value of 0.55, indicating that IgG protein is moderately hydrophobic. Accordingly, the RH scales of the reference proteins agree with those of the reference results (Johnson et al., 2017), confirming and validating the modified method of characterizing proteins by their surface hydrophobicity.

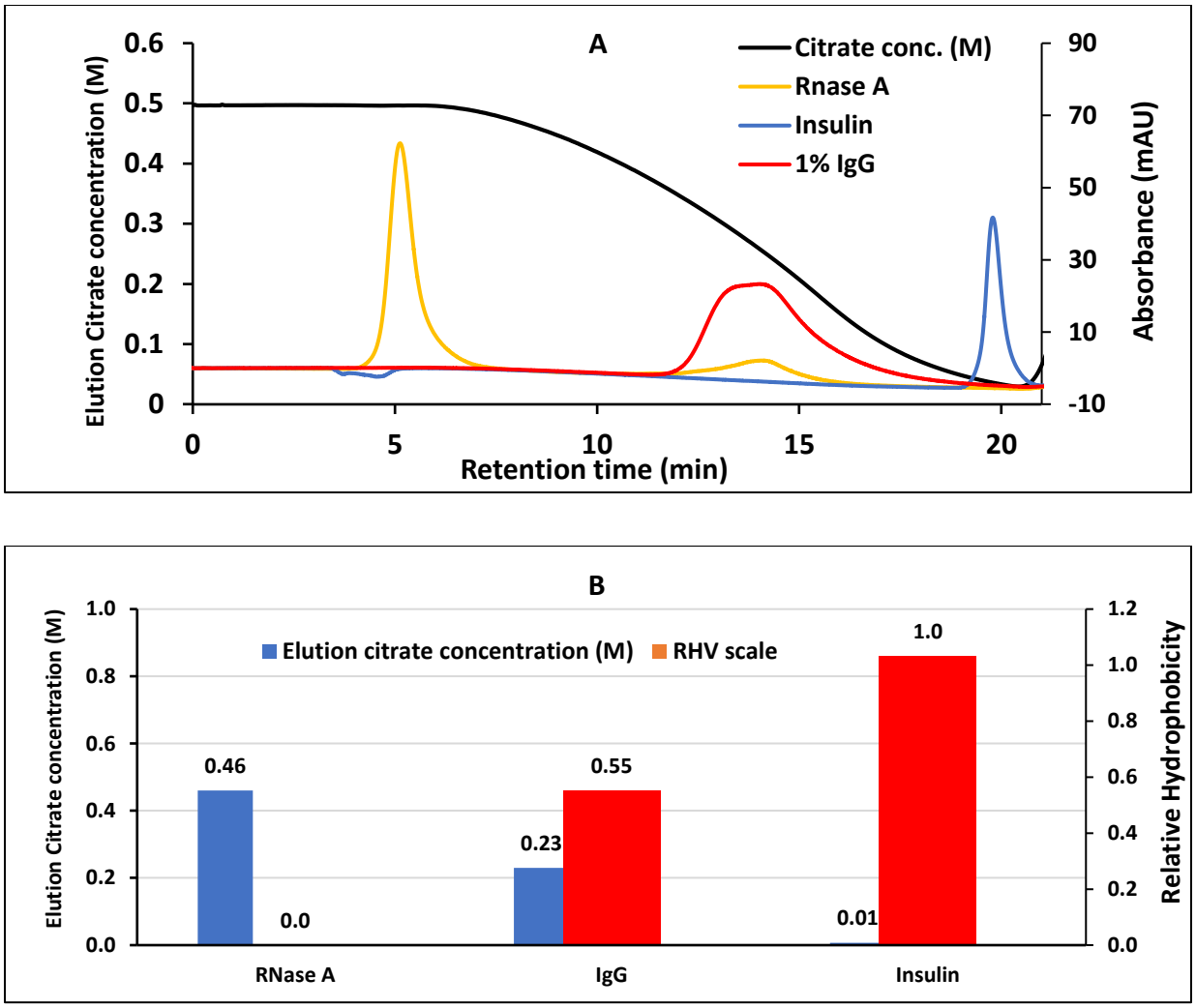

Figure 2.10 Chromatograms of IgG for determination of its relative hydrophobicity values and scales **(A)** Chromatogram of IgG in comparison to standard. **(B)** Relative hydrophobicity values for IgG sample and protein standard.

2.4 Conclusions

The experimental data obtained in this study clearly demonstrate that different concentrations of IgG can have dramatically different fouling characteristics. The differences in fouling behavior seem to be related to differences in the concentration of IgG, with highly fouling solutions containing more conformationally altered or aggregated IgG. These fouling species can be removed from the IgG solutions by prefiltration. It is possible to improve the filterability of IgG through a virus filter by prefiltration with the appropriate type of prefilter.

VPF and 75N prefilters did not provide much benefit in improving the filtrate flux at high concentrations of IgG solution and virus filter fouling was very highly correlated with the concentration of IgG dimers and other high molecular wight species in the IgG solution as determined by SEC chromatography.

The second run with BioEx filter showed less fouling and significant flux improvement because some of the fouling species were captured in the first run. The application of post-filtration buffer flush under different conditions described reversible fouling mechanisms since aggregated biomolecules could be reversed by applying a buffer flush and released into filterable molecules by desorption and resolubilization. The findings of this study contribute to a better understanding of virus filter fouling and guide mitigation strategies to enhance and reduce costs associated with Ab filtration.

CHAPTER 3: The Impact of Protein-Protein Interactions on Filtrate Flux with Highly Concentrated mAb C

3.1 Introduction

Over the past 20 years, recombinant protein production efficiency has improved dramatically. Improvements in cell culture technology, such as improved production media and feeding strategies, have increased peak cell densities, creating significant challenges for the downstream purification process (Kelley, 2007). A virus filtration step can often pose a challenge to the high concentrations of monoclonal antibodies (mAbs) obtained during cultivation of mammalian cells (Troccoli et al., 1998; Wickramasighe et al., 2019). Furthermore, virus filtration is gaining interest as part of the final fill-finish operation (along with the sterile filtration), which would offer both added protection against virus contamination and eliminate the need for a separate virus filtration operation (Isu et al., 2022).

Virus filtration uses ultrafiltration membranes with 19±2 nm pore size to remove any virus particles while retaining virus-free product within the permeate (Sofer et al., 2005). It is well known that virus filters are subjected to fouling easily despite having many advantages; resulting in flux decline, reduced capacity, and significant increases in membrane area and processing time required. To mitigate fouling, it is critical to understand the fouling mechanism of a virus filter.

There is evidence that mAb solution's properties (pI, hydrophobicity, net charge, oligomer forms), buffer conditions, membrane material, and operating pressure may influence membrane performance (Namila et al., 2019). In addition, due to the propensity of proteins to aggregate at higher concentrations, the capacity and fouling behavior of virus filtration may be compromised by reversible and possibly irreversible aggregate formation and increased

interaction between the product and membrane. As it was observed that when the levels of high molecular weight species (HMWS) are higher the filter flux was significantly decreased (Bieberbach et al., 2019; Jezek et al., 2011).

Reversible aggregates are soluble aggregations in which the associated product monomers are not significantly denatured (Li et al., 2016; Vázquez-Rey & Lang, 2011; Wang, 2005). Soluble aggregates are formed when product molecules interact via hydrogen bonding, electrostatic forces, or van der Waals forces (Leckband & Israelachvili, 2001; Wöll & Hubbuch, 2020). The probability of producing irreversible aggregates is also markedly increased with denatured product monomers and is proportional to the protein concentration. When a product is denatured or conformationally deformed, significant hydrophobic interactions will occur between its molecules as well as the protein and membrane (Philo & Arakawa, 2009; Wöll & Hubbuch, 2020). Consequently, reversible and irreversible aggregation of proteins depends on the product and solution condition, as each protein has its unique conformational stability at each specific solution condition.

As the solution pH and ionic strength affect electrostatic and hydrophobic interactions between protein-protein and protein-substrate, they are critical variables in downstream purification of mAbs. In addition, protein-protein association is probably different at high product concentrations because of the changing van der Waals and electrostatic interactions (Bieberbach et al., 2019; Wickramasinghe et al., 2010).

The use of prefilters is expected to improve membrane life and virus retention by decreasing membrane plugging (Billups et al., 2021; Bolton et al., 2006). The separation-active layer of virus filtration membranes typically has pores with a size of around 20 nm. It was reported that small aggregates with a diameter less than 50 nm could not be removed by 0.1 or

0.22 μm size exclusion filters but can block virus filter pores and play a significant role in membrane fouling (Wickramasighe et al., 2019). It may be necessary to remove these soluble aggregates using adsorptive prefilters (Ion Exchange (IEX) or Hydrophobic Interaction Chromatography (HIC)) if their size exceeds the 20 nm size cutoff of most parvovirus filters. Oligomers with molecular weights between 600-1500 kDa that cannot be removed by 0.22 μm size-exclusion prefilters have been demonstrated to be effectively reduced by adsorptive prefilters (Isu et al., 2022). Using IEX membranes as adsorptive prefilters, biotherapeutic products can be prefiltered to remove aggregates and charge variants prone to aggregation (Kahle et al., 2019; Yigzaw et al., 2009). Prefiltration with hydrophobic interaction chromatography (HIC) was also used to remove aggregates and denatured mAbs by taking advantage of the hydrophobicity difference between native conformation mAbs and aggregates or denatured mAbs (King et al., 2018).

To ensure the quality and safety of drug products, antibodies with a variety of size, charge, and hydrophobicity are characterized at different stages of their production. It has been found that Size Exclusion Chromatography (SEC) can be used to determine of irreversible foulants species with high molecular weight (HMW) in native conditions. CE-SDS has been shown to be more reliable in quantifying low molecular weight species (LMWS) under denaturing conditions (Kahle et al., 2019). Reversible monomer association can also be identified by determining the Dynamic Light Scattering (DLS) interaction parameter k_D, which describes protein-protein interactions that are concentration-dependent (Bieberbach et al., 2019; Nobbmann et al., 2007). Therefore, the more negative value of k_D indicates positive intermolecular attraction, while a positive value indicates repulsion. As shown by an earlier study, the diffusion interaction parameter, k_D is strongly influenced by the solution condition and

can be correlated with the average flux values (Namila, 2020). As product titer increases, the diffusion coefficient decreases, showing that there is an increase in product interactions. However, it is unclear how these attractive intermolecular interactions cause the large flux decline, and there is currently no clear understanding of how to effectively reduce these interactions to enable effective virus filtration at high antibody titers. Therefore, the overall goal of this study is to present data on the virus filtration performance of mAb solutions at high concentrations above ≥50 g/L and will also show the impact of the protein-protein interactions and their aggregates on the filtrate flux during virus filtration. HIC and IEX membranes are examined as prefilters for the Viresolve® Pro. Different characterization techniques are used to explain fouling mechanisms at the molecular level.

3.2 Material and Methods

3.2.1 Materials

Reagents used include sodium phosphate monobasic monohydrate (ACS reagent, ≥98%) and anhydrous sodium phosphate dibasic from Millipore Sigma (Reagent Plus®, ≥99.0%) (St. Louis, MO), tris base (biotechnology grade) from G-BioSciences (St. Louis, MO), L-Arginine (reagent grade, ≥98.0%)) from Sigma- Aldrich and Sodium chloride (molecular biology grade > 98% purity).

SDS-MW gel buffer, acidic and basic wash solutions, MW ladder, 10 kDa internal standard, and Tris/SDS sample buffer (pH 9.0) were purchased as a kit from Sciex Separations (Framingham, MA). Iodoacetamide (IAM) (≥98 %) was purchased from VWR Life science (Radnor, PA).

Nalgene™ rapid-flow™ bottle top filters (0.2µm) were sourced from ThermoFisher Scientific (Waltham, MA). Other prefilters used in this study were Sartobind® Phenyl nano (3

mL), and Sartobind® S nano (3 mL, 8 mm bed height) provided by Sartorius (Göttingen, Germany). The selected virus filters were Viresolve® Pro filter (3.1 cm^2) provided by EMD Millipore (Billerica, MA). TangenX Sius-LS TFF Cassettes LSn (30 kDa MWCO, mPES, 0.1 m^2) was provided by Repligen (Marlborough, MA).

3.2.2 Protein Feed Solution Preparation and Characterization

An industrial monoclonal antibody (mAb C) was provided by a biopharmaceutical company with a concentration of approximately 7 g/L and was kept frozen at -80 °C until used.

mAb C was thawed by first equilibrating for 1 day at -20 °C and then 2 days at 4 °C. Before each set of virus filtration experiments, the proteins were first buffer exchanged into the desired solution using tangential flow filtration (Ultrafiltration and Diafiltration/UFDF). The buffer pH and conductivity were measured using Thermo Scientific Orion STAR A215 pH/Conductivity Benchtop Meter from ThermoFisher Scientific (Waltham, MA) and adjusted as needed by adding small amounts of 1 M solutions of the appropriate acid or base (e.g., HCl or NaOH). Following preparation, the solutions were filtered through a 0.2µm bottle top filter to remove any salt, particulates, or insoluble protein aggregates formed during preparation.

In two experiments, the protein was the first buffer exchanged into 50 mM tris-acetate (pH 7.2) and the second buffer exchanged into 50 mM sodium phosphate (pH 7.2). Buffer-exchange was performed by diafiltration of 1-1.8 L of protein stock at approximately 7 g/L protein for 7 diafiltration volumes using a TangenX Sius-LS TFF Cassettes LSn (30 kDa MWCO, mPES, 0.1 m^2) in Millipore Pellicon® Mini Cassette Holder with a SARTOFLOW® Slice 200 Benchtop Crossflow System provided by (Sartorius AG, Göttingen, Germany) at 15 psi transmembrane pressure (TMP), and 400 mL/min flow rate. Then the protein was concentrated to approximately 50 g/L. The mAb concentrations were then diluted with respective

buffers to reach the target concentrations (1,2,5,10,25, and 50 g/L). In order to store the protein solution for longer periods, 50 mL aliquots were frozen and kept at -80°C. The aliquots were thawed using the same method as described previously. Following thawing, the proteins were stored at 4°C for up to one week.

Measurement of protein concentration and turbidity was performed by measuring the absorption at 280 nm and 340 nm, respectively, using Genesys 10 UV scanning system (Waltham, MA) with VWR quartz spectrophotometer cell (path length 1 cm) (West Chester, PA).

3.2.3 Protein Filtration

Prior to filtration, protein solutions were first prefiltered with 0.2 μm bottle top filters to remove any large aggregates or hydrophobic foulants. VPro virus filter was initially wetted with Deionized water filtered with 0.2 μm bottle-top filter into the Planova pressure reservoir (Asahi Kasei, Japan) by closing the outlet and opening the vent under 1-2 psi with the pressure controlled by Ashcroft pressure gauge (Part number: EW-68334-15; 0-100 psi, resolution 0.1, accuracy ± 0.5 full-scale). Following that, filters were flushed with 100 L/m² of DI water, followed by 100 L/m² of equilibration buffer to ensure complete wetting and to remove any air bubbles trapped in the system. Industrial grade nitrogen at 10.0 psi was used to pressurize the feed reservoir. Prefiltered protein solution was gently poured down the vessel wall. Filtration was conducted by closing the feed side vent, sending the gas to the filter, and filtering at constant pressure of 30 psi.

A Mettler Toledo scale (Columbus, OH) was connected to BalanceLink software to record the cumulative weight of the filtrate every minute. The data collected was used to

calculate the filtrate flux. The protein concentration of each fraction of the feed and filtrate was determined by measuring the absorbance at 280 nm with a spectrophotometer.

HIC and IEX-S prefiltration of 47 g/L and 10 g/L mAb C was performed using the Sartobind phenyl and Sartobind S membrane adsorbers in the decoupled prefiltration mode before virus filtration. Prefilters were installed on an AKTA- FPLC from Amersham Pharmacia Biotech (Uppsala, Sweden) with FRAC-950 fraction collector using the associated Control 2-Mindy software. In this experiment, conductivity and absorbance were measured at 280 nm. Prior to connect the membranes, the FPLC system was flushed with filtered DI water. Membrane was installed in an upright position in the process flow. Over 5 minutes, the membrane was wetted with DI water filtered with 0.2 μm bottle-top filter in reverse flow by gradually increasing the flow rate from 0.2 mL/min to 1.0 mL/min to minimize the possibility of air entering the membrane devices. Following this, the devices were equilibrated in the forward flow configuration at 1.0 mL/min with the sample buffer (50 mM Tris at pH 7.2) for 30 min or until the conductivity and UV absorbance at 280 nm were stable.

In this experiment, the 0.2 μm filtered protein sample solution was loaded onto the membrane device for 10 minutes at a flow rate of 1.0 mL/min. After wash the membrane with feed buffer, the protein was eluted with 150 mM Arginine, pH 7.2, at 1.0 mL/min. An elution fraction and washing fraction were collected and the volume was calculated. At 280 nm, UV absorbance was measured to determine protein concentration in each fraction. The elution fraction was used immediately for virus filtration using Viresolve® Pro membrane.

3.2.4 Size Exclusion Chromatography

The size exclusion chromatography (SEC) technique with a TSK Gel 3000 SWXL column (30 cm L 7.8 mm ID., Tosoh Bioscience, LLC) was performed on a high-performance

liquid chromatography instrument HPLC (Agilent 1260 Infinity Quaternary LC) manufactured by Agilent Technologies (Santa Clara, CA) using a TSK Gel 3000 SWXL column (30 cm L 7.8 mm ID., Tosoh Bioscience, LLC) consisting of a quaternary pump with degasser, an autosampler with a cooling unit, a column oven, and a DAD detector. The samples were filtered through a polyethersulfone (PES) syringe filter prior to analysis. The separation was carried out at a flow rate of 1.0 mL/min with a sample injection volume of 10 μL. The mobile phase 50 mM Tris buffer at pH 7.2 for mAb samples, filtered with a 0.2 μm bottle top filter. UV absorbance peaks were detected at 280 and 220 nm to determine the relative amounts of monomer and product variants.

3.2.5 Dynamic Light Scattering and Diffusion Interaction Parameter

Dynamic light scattering (DLS), a method for the investigation of the hydrodynamic radius and diffusion coefficient of the mAb was conducted with a Delsa™ Nano particle size analyzer (Beckman Coulter, Brea, CA). Protein solutions were filtered with a 0.2 μm polyethersulfone (PES) syringe filter before transferring a 1 mL aliquot into a disposable polystyrene cuvette with a 1 cm pathlength (BrandTech, Essex, CT). Three repeats with different aliquots were carried out for each sample and 500 acquisitions in each repeat were used to record the DLS data. The software was used to analyze the collected data, which resulted in a mean hydrodynamic dynamic diameter and a diffusion coefficient for the mAb at each concentration in each solution condition. The diffusion coefficient and hydrodynamic radius of a molecule can be calculated using the DLS intensity data. A diffusion interaction parameter, kD, was determined by using the following formula:

$$D_t = D_0 (1 + k_D c) \quad \text{(Equation 3.1)}$$

D_t is the observed diffusion coefficient, D_0 is the self-diffusion coefficient at infinite dilution, k_D is the diffusion interaction parameter, and c is the antibody concentration. As a result of non-specific interactions between proteins involving hydrophobic and charged residues, D_t acts as a function of the concentration (Kenrick & Some, 2014).

3.2.6 Capillary Electrophoresis –SDS Molecular weight (CE-SDS MW) analysis

mAb C were analyzed using the capillary electrophoresis instrument (PA 800 plus) to identify MW variants, charge variants, glycovariants, and impurities. The instrument parameters included a 50 μM ID and a 30 cm total length of bare fused silica capillary which was filled with the SDS-MW gel-buffer system.

Samples were diluted with CE-SDS Sample Buffer to a final concentration of 1 mg/mL. Then, 2 μL of Internal Standard was added to each sample. 5 μL of a 250 mM stock solution of the alkylating agent IAM was added to each sample to block disulfide scrambling or exchange. Samples were denatured at 70◦C for 3 minutes and mixed by vortex, cooled on ice for 5 minutes and mixed by vortex. The samples were then transferred to 96-well plates and centrifuged at 1000 x g for 10 minutes. Up to 72 samples can be loaded at once. Characterization takes place sequentially based on the programmed software instructions. The data acquisition and processing were carried out using the 32Karat software package.

3.3 Results and Discussion

3.3.1 Virus Filtration Results Using Monoclonal antibodies mAb C

3.3.1.1 Viresolve® Pro Filtration without Prefiltration

Viresolve® Pro was used to evaluate the filtrate flux in highly concentrated mAb C in various solution conditions at pH 7.2 with no prefiltration. mAb solution was filtered with a 0.2 μm sterile filter. According to the filter manufacturer's recommendation, the filtration was

performed at 210 kPa (30 psi). The results are plotted as normalized fluxes in relation to volumetric throughput Figure 2.1. The data points represent the average of the flux measured every 5 minutes. A significant fouling of the virus filter was observed at highly concentrated mAb after UF/DF in both buffer conditions. The filter crashed immediately at the beginning of the filtration with ~47 g/L mAb C and the overall throughput was less than 10 L/m² in phosphate buffer while it reached to more than 10 L/m² in tris buffer. The throughput was less than 30 L/m² in phosphate buffer with ~23 g/L and reached to more than 30 L/m² in tris buffer. However, the least degree of flux drop (40%) was seen at ~8 g/L in tris buffer, while in phosphate buffer, significant fouling was observed at this concentration, with the throughput reaching over 50 L/m². Filter fouling is found to be strongly affected by the product concentration. This is indicating that a significant fouling decay with the highly concentrated mAb occur due to the presence of aggregates/impurities that cannot be removed with 0.2 μm prefilter generate during UF/DF to concentrate the protein from ~7 g/L to ~50 g/L. In general, higher protein concentrations can reduce the average process flux and product throughput during virus filtration. The level of impact will depend on the interaction between the filter and the solution components (Kern & Krishnan, 2006). In addition, the properties of mAbs are highly dependent on the buffer conditions used in their formulation. A specific buffer type and composition may be found to inhibit aggregation and mitigate fouling of virus filters during high throughput screening of mAbs (Isu, 2022). Protein recovery and mass balance for the VPro filtration fractions at both buffer conditions are shown in Table 2.1 below.

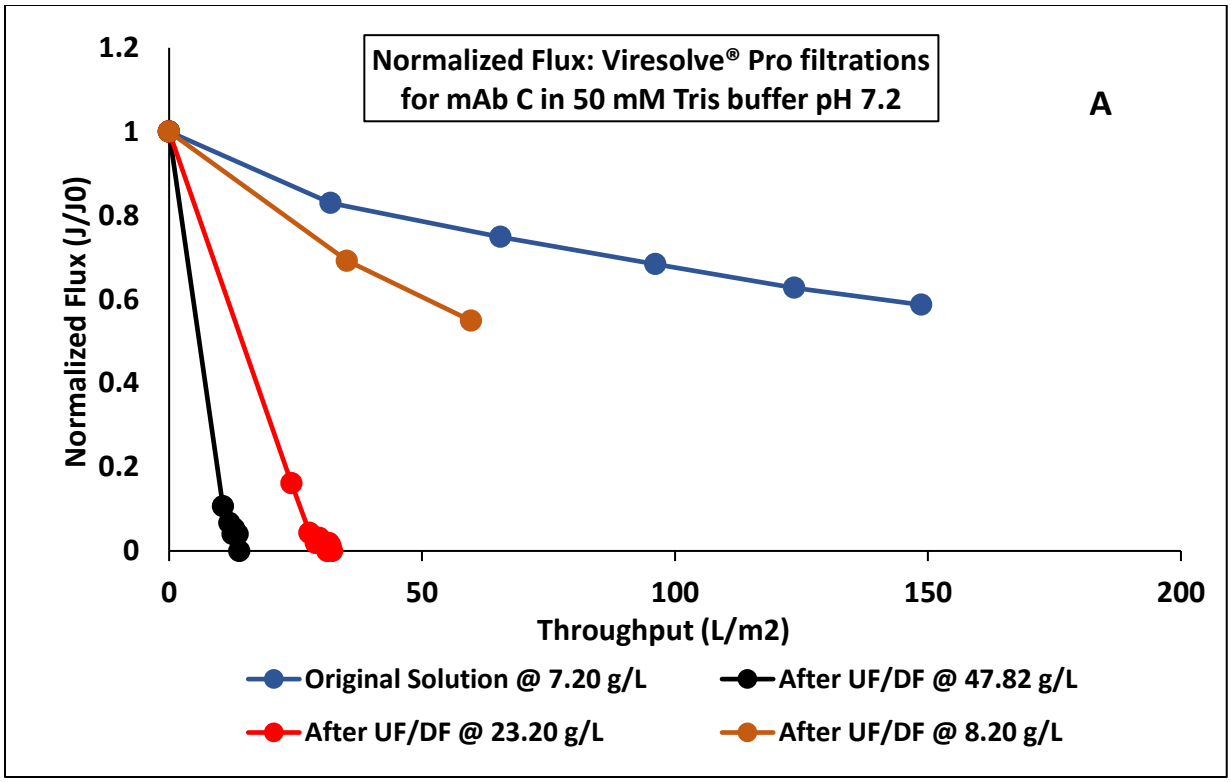

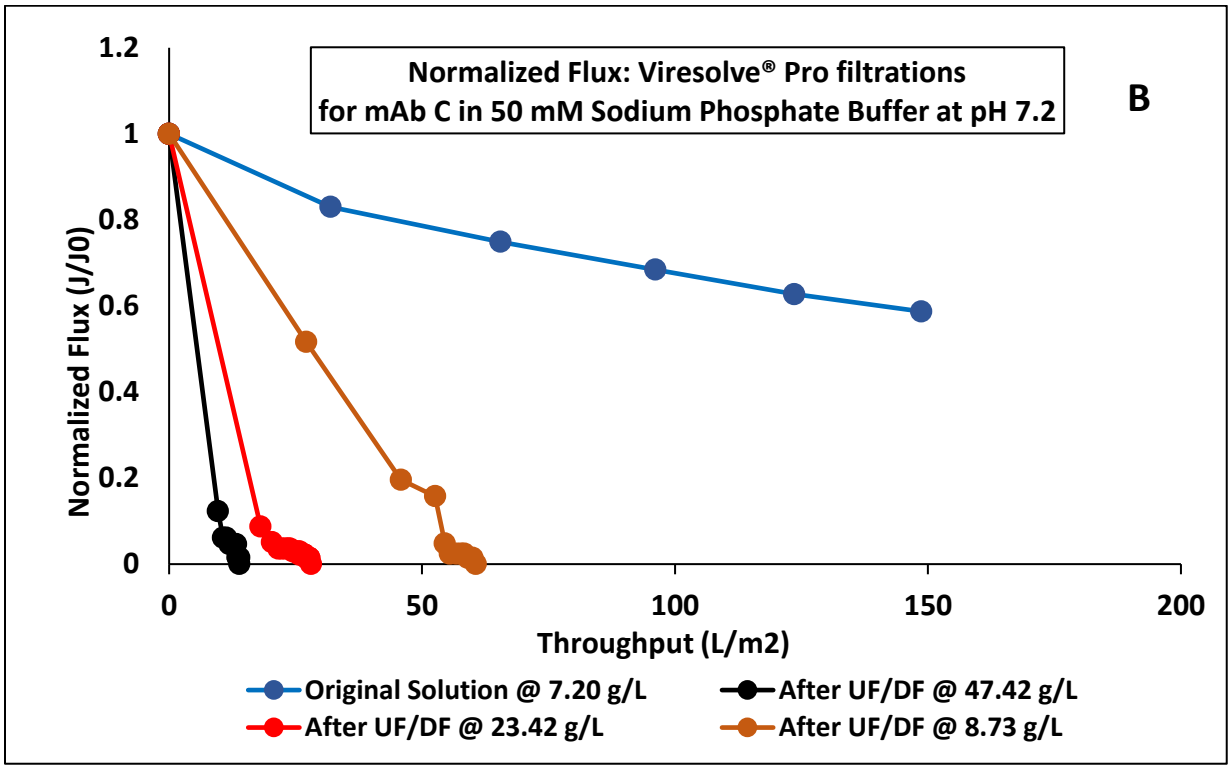

Figure 3.1 Virus filtration experiments with Viresolve® Pro were performed for different concentrations of mAb C before and after UF/DF in 50 mM tris buffer **(A)** and 50 mM Sodium phosphate buffer **(B)** at pH 7.2.

Table 3.1 Mass Balance for VPro filtration mAb C fractions in 50 mM tris buffer and 50 mM Sodium phosphate buffer at pH 7.2.

VPro Filtration of mAb C in in 50 mM tris, pH7.2				
Tube 1	**Dilution factor**	**Abs @ 280 nm**	**Concentration (mg/mL)**	**Mass (mg)**
mAb C After UF/DF	**x80**	**0.84**	**47.82**	**210.4**
VPro filtrate	**x50**	**0.71**	**25.50**	**112.2**
Protein recovery	**53.32%**			
Tube 2	**Dilution factor**	**Abs @ 280 nm**	**Concentration (mg/mL)**	**Mass (mg)**
Feed	**x40**	**0.81**	**23.2**	**232.00**
VPro Filtrate	**x30**	**0.77**	**16.70**	**167.00**
Protein recovery	**71.98%**			
Tube 3	**Dilution factor**	**Abs @ 280 nm**	**Concentration (mg/mL)**	**Mass (mg)**
Feed	**x15**	**0.76**	**8.20**	**174.6**
VPro Filtrate	**x10**	**0.97**	**6.70**	**148.74**
Protein recovery	**85.18%**			
VPro Filtration of mAb C in 50 mM Sodium phosphate, pH7.2	**Dilution factor**	**Abs @ 280 nm**	**Concentration (mg/mL)**	**Mass (mg)**
Tube 1				
mAb C After UF/DF	**x80**	**0.84**	**47.42**	**230.95**
VPro filtrate	**x50**	**0.64**	**22.85**	**115.42**
Protein recovery	**50.00%**			
Tube 2	**Dilution factor**	**Abs @ 280 nm**	**Concentration (mg/mL)**	**Mass (mg)**
Feed	**x40**	**0.79**	**23.42**	**238.60**
VPro Filtrate	**x30**	**0.71**	**15.71**	**177.70**
Protein recovery	**74.47%**			
Tube 3	**Dilution factor**	**Abs @ 280 nm**	**Concentration (mg/mL)**	**Mass (mg)**
Feed	**x15**	**0.79**	**8.73**	**209.92**
VPro Filtrate	**x10**	**0.97**	**7.14**	**183.296**
Protein recovery	**87.31%**			

3.3.1.2 Viresolve® Pro Filtration of mAb C with Adsorptive Prefiltration (Sartobind Phenyl, and Sartobind S)

Adsorptive prefiltration was carried out in flowthrough mode with HIC and IEX-S prefilters, followed by virus filtration. Figure 2.2 below shows the chromatogram with HIC and IEX-S prefilters for mAb C in 50 mM tris buffer at pH 7.2. As can be seen from the chromatogram, the flowthrough fraction represents a broad peak while there is smaller elution peak area in the HIC compared to the IEX-S prefilter, which is much larger. It is proposed that the HIC prefilter is more effective than ion-exchange mechanism adsorptive prefilters in removing hydrophobicity-induced foulant species (possibly denatured mAbs).

Virus filtration with Viresolve® Pro filtration device was done after HIC and IEX-S prefiltration of mAb C solution. As can be seen in Figure 2.3a significant flux decay was observed at the end of ~13 L/m² throughput while after prefiltration the flux decay was observed at the end of ~62 L/m² throughput. IEX-S prefiltration shows less than 10 percent flux decay compared to 30 percent flux decay without prefiltration. Table 2.2 below shows the mass balance of the VPro filtration fractions where greater than 95% mAb C recovery was achieved.

Prefiltration using HIC and IEX-S filter improved the performance of VPro filters. This is indicating that adsorptive prefilters removed product variants, aggregates, and other residual impurities. A similar observation has been reported previously by Isu (2022). Brown et al. (2010) also found that Ion exchange membrane adsorbers can improve the virus filter throughput of mAbs.

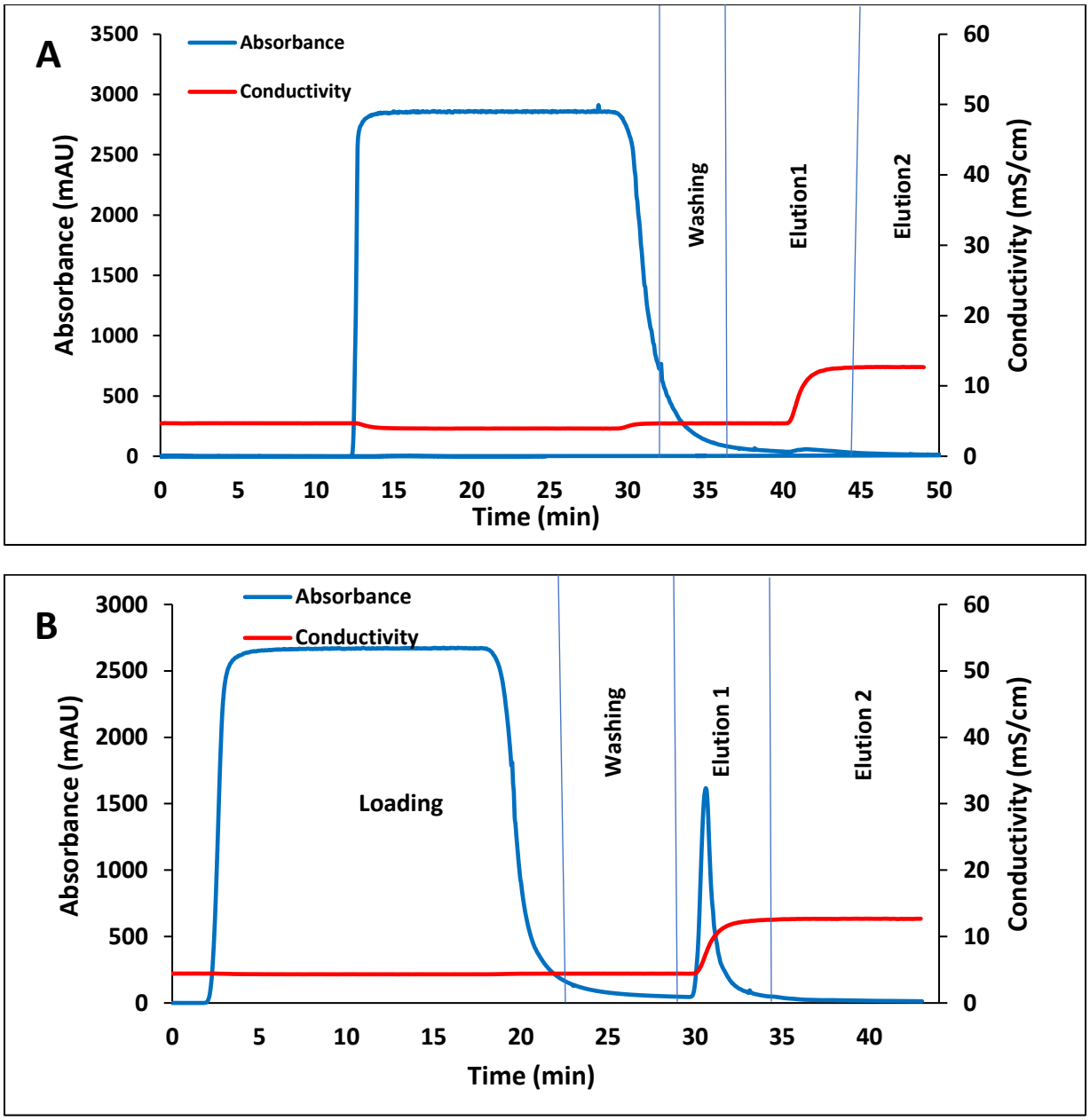

Figure 3.2 (A) Chromatogram for HIC Prefiltration of 47 g/L mAb C in 50 mM tris buffer at pH 7.2. **(B)** Chromatogram for IEX-S Prefiltration of 10 g/L mAb C in 50 mM tris buffer at pH 7.2.

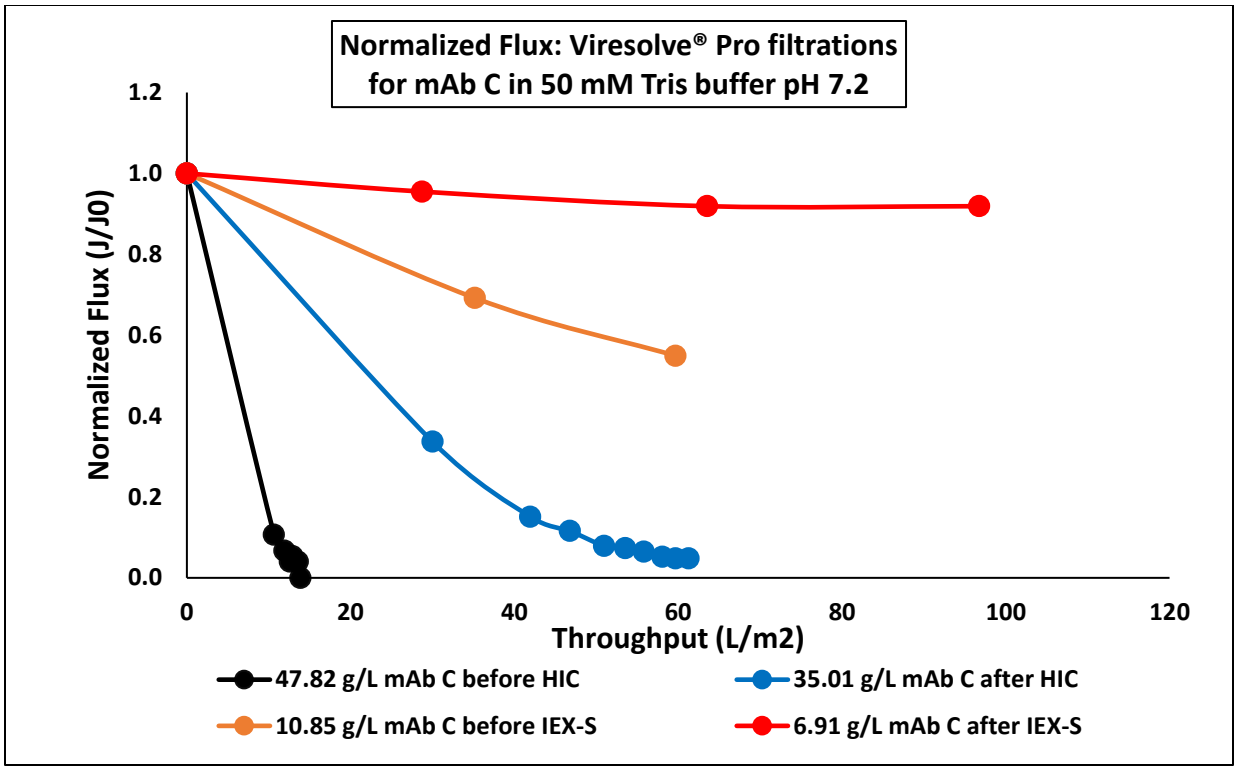

Figure 3.3 VPro Filtration of mAb C in 50 mM tris buffer at pH 7.2 before and after HIC and IEX-S prefiltration.

Table 3.2 Mass Balance for VPro filtration mAb C fractions after prefiltration in 50 mM tris buffer at pH 7.2.

Tube 1	Dilution factor	Abs @ 280nm	Concentration (mg/mL)	Mass (mg)
mAb C before prefiltration	x80	0.83	47.82	408.00
HIC filtrate	x60	0.81	35.01	700.20
VPro filtrate	x60	0.81	34.84	661.96
Protein recovery	94.53%			
Tube 2	Dilution factor	Abs @ 280nm	Concentration (mg/mL)	Mass (mg)
mAb C before prefiltration	x20	0.76	10.85	379.75
IEX S filtrate	x10	0.96	6.91	248.76
VPro filtrate	x10	0.95	6.80	231.20
Buffer chase		0.13	0.096	1.24
Protein recovery	94.18%			

3.3.2 Characterization of mAb C

3.3.2.1 Turbidity measurements for mAb C

The protein solution turbidity was determined by measuring the optical density of the solution at 340 nm wavelength. Turbidity data shows particle propensity or molecule colloidal stability (Saluja et al., 2010). As is seen in Figure 2.4 higher turbidity is associated with more protein aggregates in the solution. The aggregate level increased with increasing concentration of protein in both buffer conditions. The filtrates all have very low aggregate species strongly suggesting that the presence of these aggregates leads to the fouling of the virus filter.

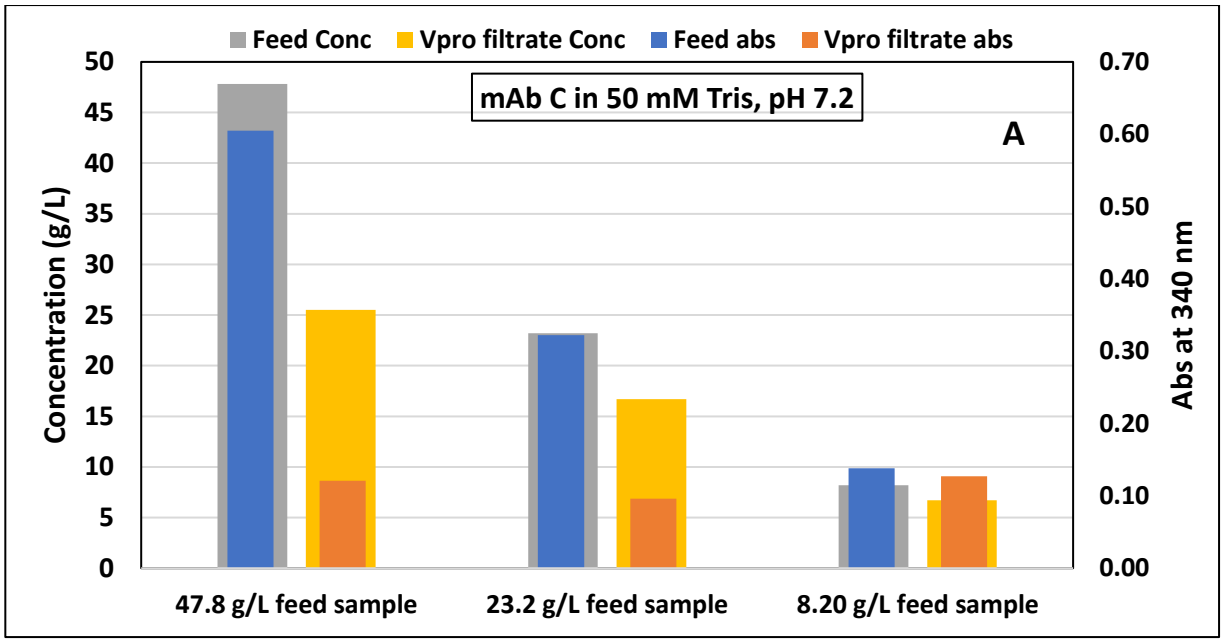

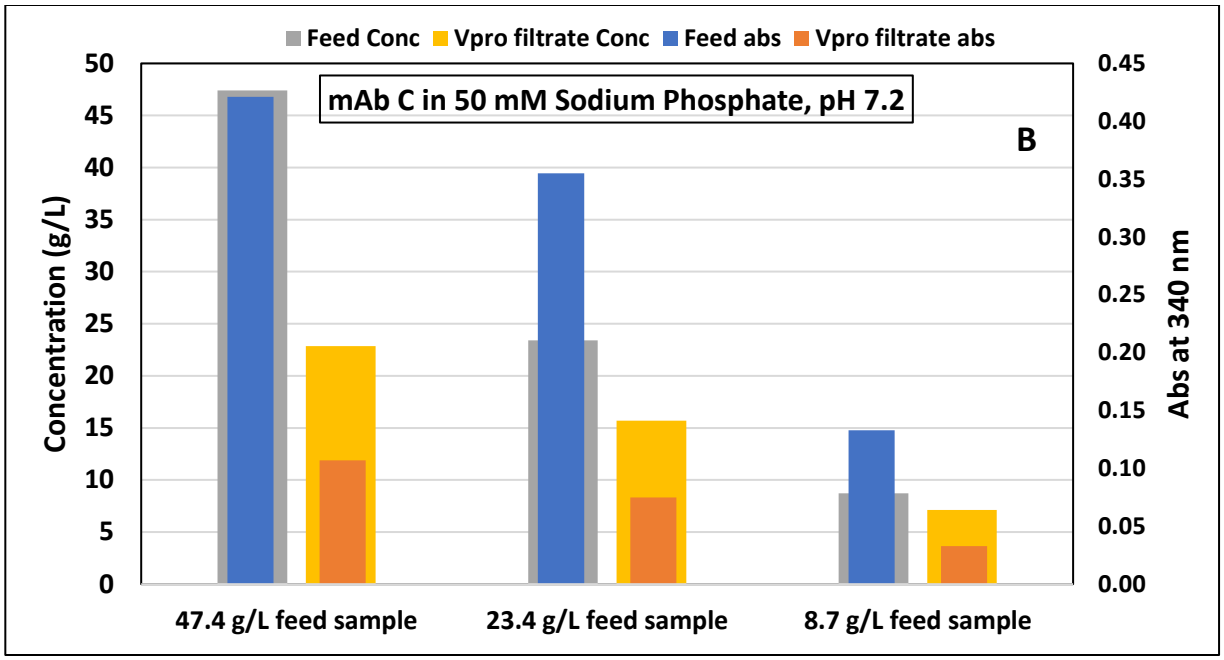

Figure 3.4 Absorbance for feed and filtrate of mAb C at different concentrations measured at 340 nm wavelength, representing the turbidity of the protein solution in two solution conditions at pH 7.2 **(A)** 50 mM tris buffer. **(B)** 50 mM sodium phosphate buffer.

3.3.2.2 Size Exclusion Chromatography Analysis of mAb C

Different concentrations of mAb C after UF/DF were analyzed using size exclusion chromatography (SEC) in 50 mM tris buffer without salt at pH 7.2. The SEC chromatogram is shown in Figure 2.5. The percentages of monomeric and dimeric mAb C were calculated and tabulated in Table 2.3. As can be seen the dimeric product does not appear to foul filters and the performance of the filtration is strongly influenced by the mAb concentration. A high concentration of high molecular weight species in the feed, that was considered to be irreversible aggregates, generally leads to reduced mAb throughput in virus filtration and filter fouling (Bieberbach et al., 2019)

Table 3.3 The percentage of monomer and dimer present in feed and filtrate of mAb C at different concentrations in 50 mM tris buffer at pH 7.2.

Sample Concentration (g/L)	Dimer %	Monomer%
Feed @47.82	2.88	97.11
Filtrate @25.50	2.74	97.25
Feed @ 23.20	2.97	97.02
Filtrate @ 16.70	4.26	95.73
Feed @ 8.20	1.40	98.59
Filtrate @ 6.70	1.82	98.17
Feed @ 5	1.50	97.59
Feed @ 2	1.18	98.81

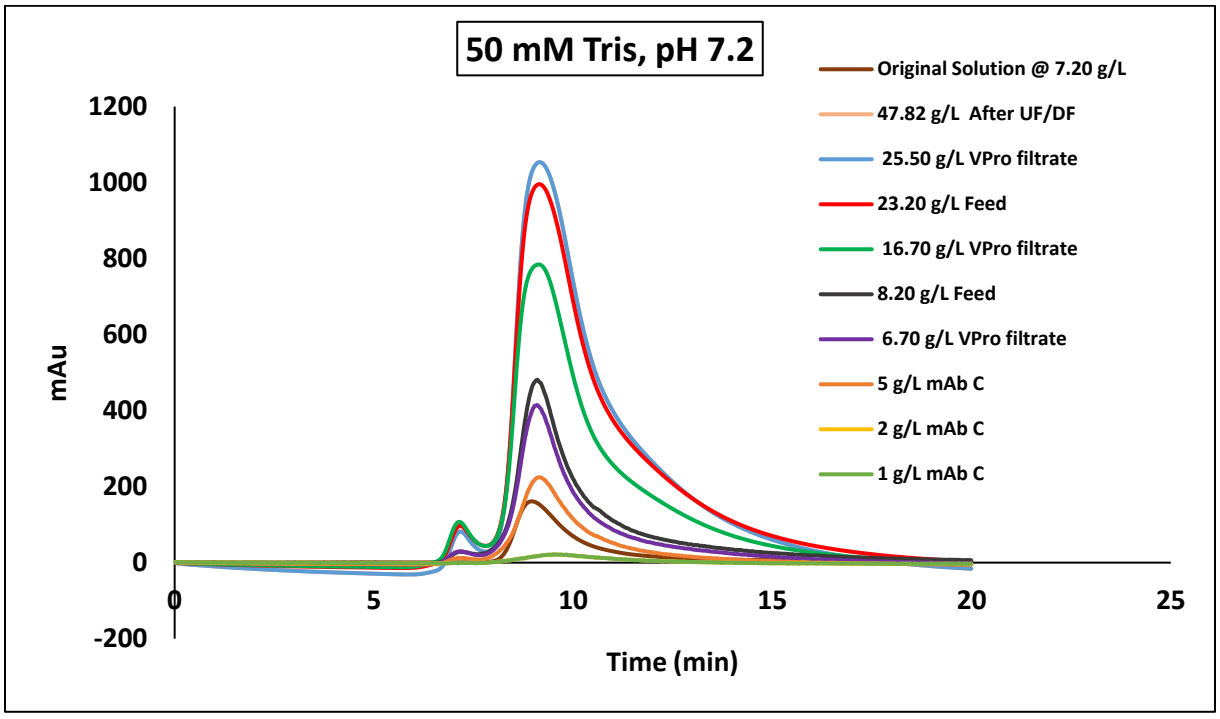

Figure 3.5 Size-Exclusion Chromatogram for feed and filtrate of mAb C at different concentrations in 50 mM tris buffer at pH 7.2.

3.3.2.3 Dynamic Light Scattering (Particle Size Analysis) of mAb C

Dynamic Light Scattering (DLS) was used to investigate the hydrodynamic diameters for mAb C fractions at different concentrations in different buffer conditions at pH 7.2. The intensity vs protein particle size measurements for mAb solution in 50 mM tris buffer is shown in Figure 2.6. and 50 mM sodium phosphate is shown in Figure 2.7. The calculated average hydrodynamics diameters for the protein concentration in 50 mM tris buffer is shown in Table 2.4. and 50 mM sodium phosphate is shown in Table 2.5. The hydrodynamic diameters of mAb C positively correlates with the mAb concentration in both conditions. As the mAb concentration goes up, the hydrodynamic diameter goes up. The hydrodynamic diameter in the feed is slightly higher than the filtrate and the highest hydrodynamic diameter is observed at 47 g/L after UF/DF. 1 g/L mAb C had the least hydrodynamic diameter. According to Wickramasinghe et al. (2019) trace aggregates that are smaller than 50 nm significantly contribute to fouling of virus filtration membranes. A virus filter can be blocked by these small aggregates with diameters less than 50 nm since they cannot be removed by 0.1 μm or 0.2 μm size exclusion filters. A virus filtration membrane typically has pores of 20 nm in its separation-active layer.

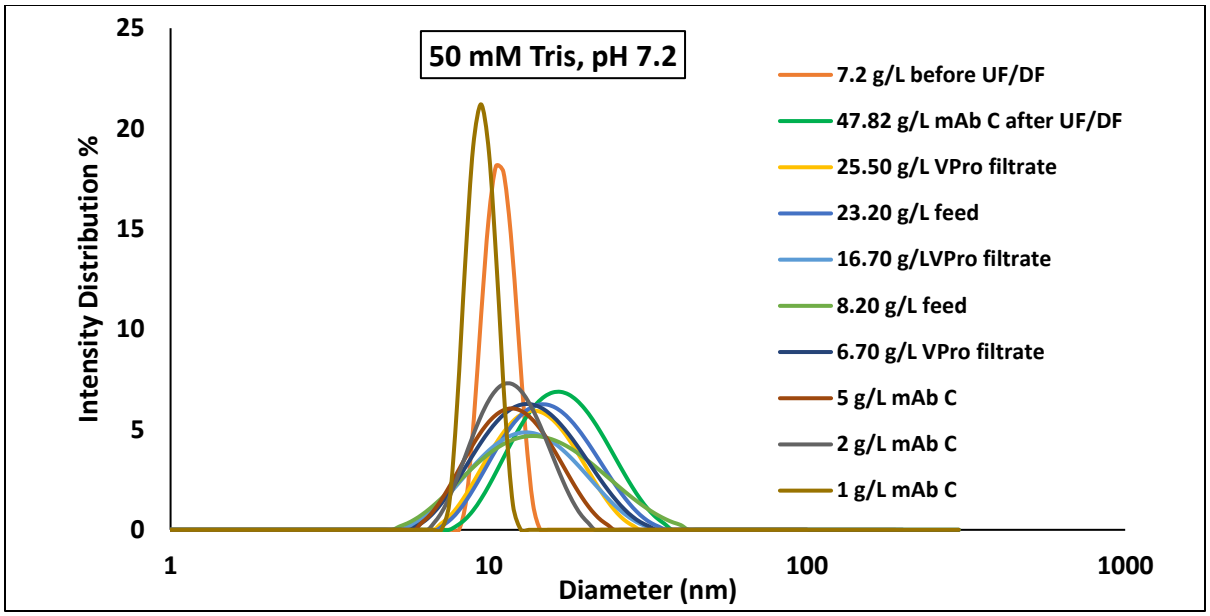

Figure 3.6 Mean hydrodynamic diameter for feed and filtrate of mAb C at different concentrations in 50 mM tris buffer at pH 7.2.

Table 3.4 The average hydrodynamic diameter (nm) for feed and filtrate of mAb C at different concentrations in 50 mM tris buffer at pH 7.2.

mAb C (50 mM Tris, pH7.2)	Diameter (nm)
7.2 g/L before UF/DF	10.8 ±1.1
47.82 g/L after UF/DF	17.6 ±5.4
25.50 g/L VPro filtrate	14.5 ±4.2
23.20 g/L Feed	15.9 ±5.1
16.70 g/L VPro filtrate	13.6 ±3.8
8.20 g/L Feed	13.3 ±4.5
6.70 g/L VPro filtrate	14.2 ±4.9
5 g/L	12.3 ±3.5
2 g/L	11.9 ±2.8
1 g/L	9.5 ±0.9

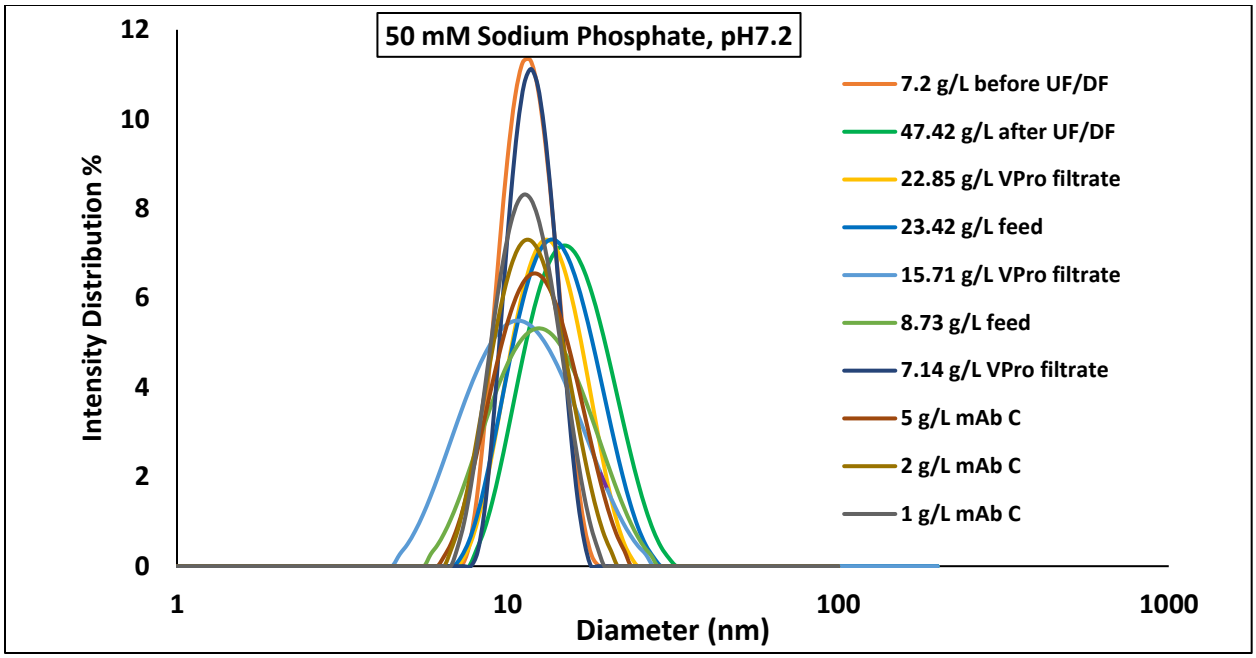

Figure 3.7 Mean hydrodynamic diameter for feed and filtrate of mAb C at different concentrations in 50 mM sodium phosphate buffer at pH 7.2.

Table 3.5 The average hydrodynamic diameter (nm) for feed and filtrate of mAb C at different concentrations in 50 mM sodium phosphate buffer at pH 7.2.

mAb C (50 mM Phosphate, pH 7.2)	Diameter (nm)
7.2 g/L before UF/DF	11.7 ± 2.0
47.42 g/L after UF/DF	15.7 ± 4.3
22.85 g/L VPro filtrate	13.5 ± 3.2
23.42 g/L Feed	14.4 ± 3.9
15.71 g/L VPro filtrate	12.1 ± 1.3
8.73 g/L Feed	13.2 ± 4.2
7.14 g/L VPro filtrate	11.9 ± 1.8
5 g/L	12.4 ± 2.9
2 g/L	13.8 ± 4.4
1 g/L	11.6 ± 2.4

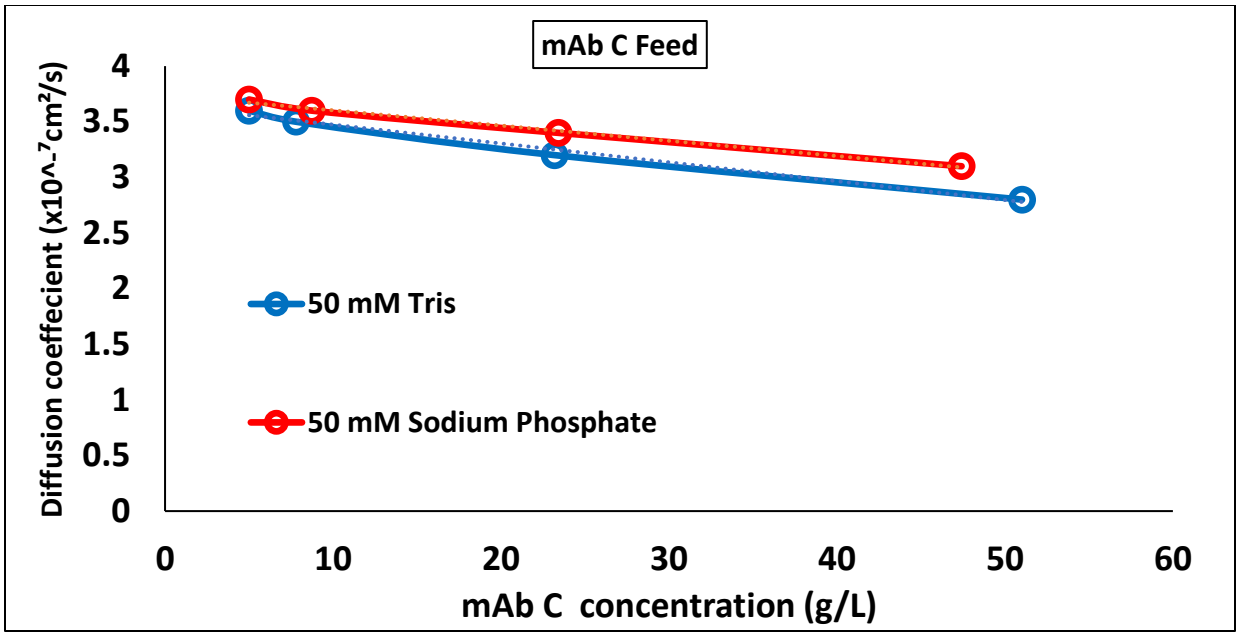

Figure 3.8 Measured diffusion coefficient as a function of mAb C feed in different buffer solutions.

Table 3.6 The calculated diffusion interaction parameter, k_D of mAb C feed in different buffer solutions.

k_D **of Feed mAb C**	
50 mM Tris	- 58.50 mL/g
50 mM Phosphate	- 41.50 mL/g

Based on the hydrodynamic radius from DLS measurement, the diffusion coefficient can be measured for mAb C at each specific solution condition. Using the equation listed in the Methods section, the diffusion interaction parameters (k_D) were calculated based on the measured diffusion coefficients against protein concentration. A recent study demonstrated that k_D could predict characteristics such as solution viscosity, colloidal stability, and protein aggregation (He et al., 2011; Saluja et al., 2010; Yadav et al., 2010)

Figures 2.8 and 2.9 show the calculated diffusion coefficient as a function of the mAb C feed and VPro filtrate concentrations in the 50 mM phosphate and 50 mM tris buffer. The two buffers modulate the protein interaction slightly differently. In both buffers, the protein tends to

have attractive interactions (diffusivity decreases with increasing mAb concentration). The magnitude of the interaction parameter was evaluated from the slopes of the two plots giving k_D = -58 mL/g for the feed and k_D= -26 mL/g for the filtrate, both for the mAb in tris buffer. The corresponding values in the sodium phosphate buffer are -41 mL/g and -30 ml/g. These results indicate that mAb C molecules in the 50 mM tris buffer tend to have a stronger tendency to aggregate compared to the 50 mM sodium phosphate buffer. This can also be seen from the hydrodynamic diameter of the protein in the two conditions. The larger hydrodynamic diameter of the protein in tris buffer indicates that the interaction of the molecules is stronger than in the phosphate buffer.

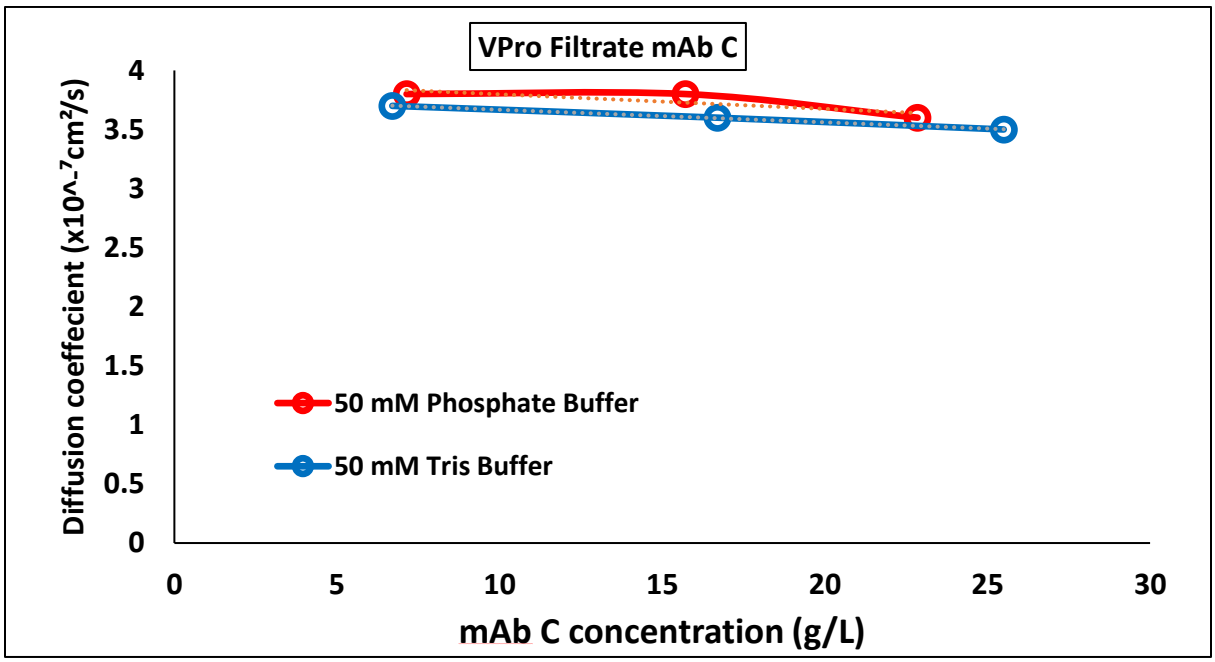

Figure 3.9 Measured diffusion coefficient as a function of mAb C VPro filtrate in different buffer solutions.

Table 3.7 The calculated diffusion interaction parameter, kD of mAb C VPro filtrate in different buffer solutions.

k_D of Filtrate mAb C	
50 mM Tris	- 26.50 ml/g
50 mM Phosphate	- 30.75 ml/g

3.3.2.4 Capillary Electrophoresis CE-SDS Analysis of mAb C

VPro, HIC and IEX-S samples were selected and characterized by CE-SDS on the PA 800 plus to detect the fine fragmentation of a mAb. Samples are left non-reduced and alkylated before being analyzed to determine the fragmentation species of mAb in their original state. It is in this context that fragmentation species consist primarily of native antibody subunits represented by light chain (L, 25 kDa), heavy chain (H, 50 kDa), heavy-light (HL, 75 kDa), heavy-heavy (H2, 100 kDa) and heavy-heavy-light (H2L, 125 kDa), which are separated from the intact mAb(H2L2, 150 kDa) and identified by their relative migration times (Wagner et al., 2020). An electropherogram of mAb shown in Figure 2.10 with non-reduced CE-SDS showed typical peaks LC, HL, HH, and HHL. The small fragment sighted at around 25 minutes co-migrates with the HH species, whereas the fragment seen at 26 minutes is a shoulder of the HHL species. It is likely, therefore, that fragments or impurities of IgG are present because CE-SDS separates species by size, so earlier eluting peaks suggest a species smaller than mAb monomer peak (eluting at ~ 28.6 min) (Duhamel et al., 2019; Wagner et al., 2020).

Figure 3.10 (A) CE-SDS Chromatogram of mAb C HIC and VPro Fractions in 50 mM sodium phosphate buffer at pH 7.0. **(B)** CE-SDS Chromatogram of mAb C IEX-S and VPro Fractions in 50 mM sodium phosphate buffer at pH 7.0.

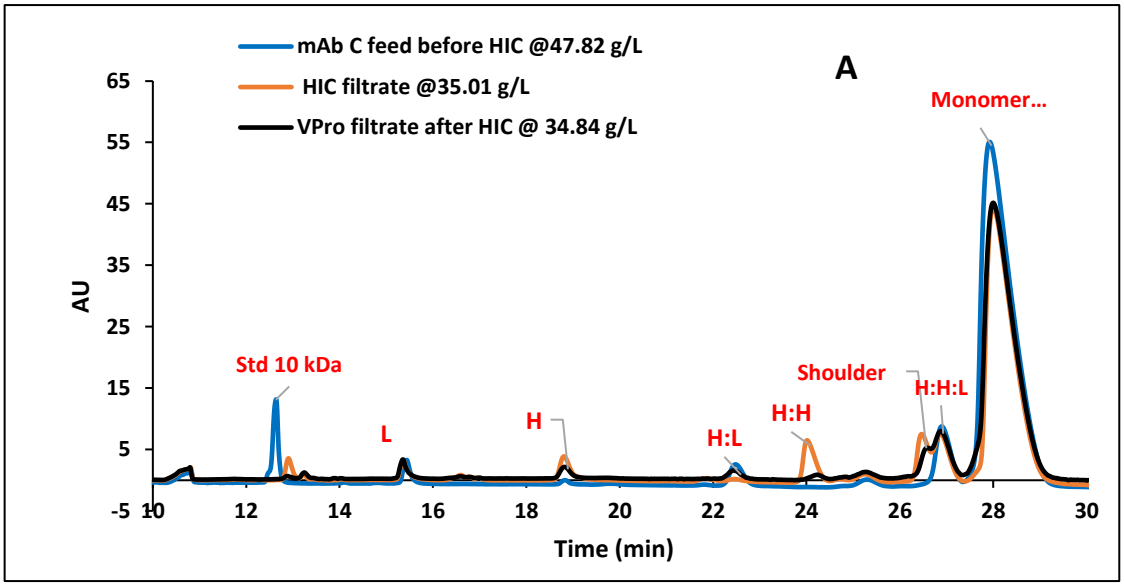

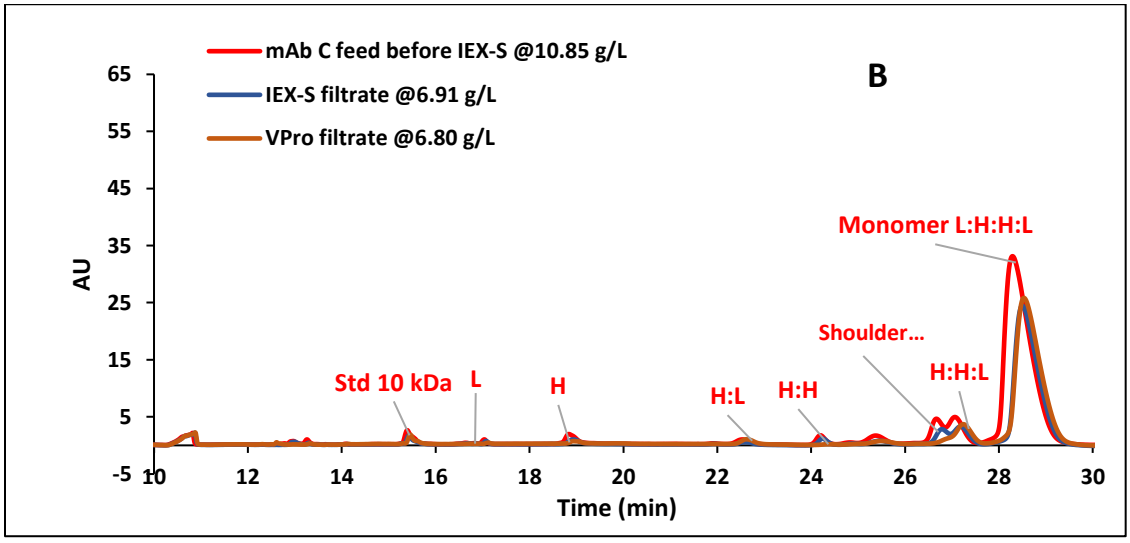

3.4 Conclusions

Filtration studies of high concentration (≥50 g/L) mAb C demonstrated that the filter fouling is strongly affected by the mAb C concentration. However, different fluxes were observed in different solution conditions. The least flux decay was observed (up to 50 L/m²) with ~10 g/L mAb C in tris buffer. It was determined that irreversible aggregates caused irreversible

plugging of membrane pores at the molecular level. The 0.2 μm prefilters were ineffective for removing these irreversible aggregates and preventing flux decay in virus filters; therefore, adsorptive prefilters are the focus in this section for mAb C. By prefiltering with adsorptive prefilters, these irreversible aggregates can be effectively removed. The diffusion interaction parameter k_D was easily determined using a DLS device, in two buffer conditions. It was used to predict characteristics like solution viscosity, colloidal stability, and protein aggregation. mAb C molecules in the 50 mM tris buffer tend to have a stronger tendency to aggregate compared to the 50 mM sodium phosphate buffer. The larger hydrodynamic diameter of the protein in tris buffer indicated that the interaction of the molecules is stronger than in the phosphate buffer. CE-SDS characterization showed small peaks of fragmented light and heavy chains. The HIC and IEX-S eluate peaks showed slightly higher peaks than the filtrate fractions.

CHAPTER 4: Conclusions and Future Direction

4.1 Conclusions and Future Direction

A primary goal of this project is to provide new insights into the factors controlling the filtration of highly concentrated proteins. An industry advisory board nominated this project, which addressed an essential need in the biopharmaceutical industry. A study has been conducted to correlate molecular properties of highly concentrated proteins in different buffer conditions with fouling behavior in virus filters and to provide robust virus removal steps during or just before fill-finish operations.

Although, the structure of IgGs and mAbs are well known, all recombinant derived molecules of these molecules have unique sources of heterogeneity attributes that could increase fouling propensity, including loss of native-state conformations, charge variation, and hydrophobicity variation. As product titers increase, protein monomeric variants could foul virus filters through adsorptive processes or by forming reversible aggregates that plug the virus filter pores. Thus, reversible and irreversible fouling species were described based on the observation of different virus filtration performances for high concentrations IgG and mAb solutions combined with buffer flush experiments.

At the molecular level, irreversible aggregates are responsible for irreversibly plugging membrane pores. The reversible fouling, however, which can be reversed by flushing a fouled virus filter with buffer, could be attributed to concentration dependent reversible protein oligomer formation, which is further enhanced by concentration polarization within the membrane structure, resulting in reduced total flux and a decelerated antibodies transport velocity.

Prefiltration before virus filtration can capture fouling species variants primarily. Through the capture of fouling mAb variants, virus filter banks can run longer with seamless operations and fewer downtimes, thereby reducing costs. The hydrophobic interaction and ion exchange chromatography membrane adsorbers were found to be very robust for mAb prefiltration in the buffer conditions evaluated for mAb C, including tris buffer at pH 7.2.

It would be useful in the future to evaluate more mAb products from additional biopharmaceutical companies so that more data can be included in the machine learning model. An emphasis can be placed on identifying mAb variants with high fouling index and create guideline for prefilter selection for virus filtration at high product titers. More work should be performed using an efficient virus filtration membrane with high capacity and high virus reduction and multimodal prefilters from multiple manufacturers.

As is shown in this thesis, the filtrate flux of a virus filter is affected by solution conditions. Thus, by optimizing mAb formulation buffer during prefiltration, biopharmaceutical companies are providing a robust template for process development, optimizing virus filter performance and reducing drug end-user costs. Virus filter manufacturers can also modify current membranes or design new materials or membranes for virus filtration at high product titers at the end of downstream purification train by understanding the nature and characteristics of principal foulants. Research is needed to improve mAb product safety and reduce the cost of producing mAbs to reduce the intravenous delivery of monoclonal antibodies to patients.

References

Aggarwal, S. (2009). What's fueling the biotech engine—2008. *Nature Biotechnology*, *27*(11), 987–993. https://doi.org/10.1038/nbt1109-987

Bakhshayeshi, M., & Zydney, A. L. (2008). Effect of Solution pH on Protein Transmission and Membrane Capacity During Virus Filtration. *Biotechnology and Bioengineering*, *100*(1), 108–117. https://doi.org/10.1002/bit.21735

Bansal, R., Gupta, S., & Rathore, A. S. (2019). Analytical Platform for Monitoring Aggregation of Monoclonal Antibody Therapeutics. *Pharmaceutical Research*, *36*(11), 152. https://doi.org/10.1007/s11095-019-2690-8

Barnard, J. G., Kahn, D., Cetlin, D., Randolph, T. W., & Carpenter, J. F. (2014). Investigations into the Fouling Mechanism of Parvovirus Filters During Filtration of Freeze-Thawed mAb Drug Substance Solutions. *Journal of Pharmaceutical Sciences*, *103*(3), 890–899. https://doi.org/10.1002/jps.23881

Barone, P. W., Wiebe, M. E., Leung, J. C., Hussein, I. T. M., Keumurian, F. J., Bouressa, J., Brussel, A., Chen, D., Chong, M., Dehghani, H., Gerentes, L., Gilbert, J., Gold, D., Kiss, R., Kreil, T. R., Labatut, R., Li, Y., Müllberg, J., Mallet, L., … Springs, S. L. (2020). Viral contamination in biologic manufacture and implications for emerging therapies. *Nature Biotechnology*, *38*(5), 563–572. https://doi.org/10.1038/s41587-020-0507-2

Belfort, G., Davisb, R. H., & Zydney, A. L. (1994). The behavior of suspensions and macromolecular solutions in crossflow microfiltration. *Journal of Membrane Science*, *96*(1–2), 1–58.

Berger, M., Shankar, V., & Vafai, A. (2002). Therapeutic Applications of Monoclonal Antibodies. *The American Journal of the Medical Sciences*, *324*(1), 14–30. https://doi.org/10.1097/00000441-200207000-00004

Bieberbach, M., Kosiol, P., Seay, A., Bennecke, M., Hansmann, B., Hepbildikler, S., & Thom, V. (2019). Investigation of Fouling Mechanisms of Virus Filters during the Filtration of Protein Solutions Using a High Throughput Filtration Screening Device. *Biotechnology Progress*, *35*(4). https://doi.org/10.1002/btpr.2776

Billups, M., Minervini, M., Holstein, M., Feroz, H., Ranjan, S., Hung, J., Bao, H., Ghose, S., Li, Z. J., & Zydney, A. L. (2021). Antibody retention by virus filtration membranes: Polarization and sieving effects. *Journal of Membrane Science*, *620*, 118884. https://doi.org/10.1016/j.memsci.2020.118884

Billups, M., Minervini, M., Holstein, M., Feroz, H., Ranjan, S., Hung, J., Bao, H., Li, Z. J., Ghose, S., & Zydney, A. L. (2022). Role of membrane structure on the filtrate flux during monoclonal antibody filtration through virus retentive membranes. *Biotechnology Progress*, *38*(2). https://doi.org/10.1002/BTPR.3231

Binabaji, E. (2015). *Ultrafiltration of Highly Concentrated Monoclonal Antibody Solutions* [Graduate Theses and Dissertations, The Pennsylvania State University]. https://www.proquest.com/docview/1710719836?pq-origsite=gscholar&fromopenview=true

Bohonak, D. M., & Zydney, A. L. (2005). Compaction and permeability effects with virus filtration membranes. *Journal of Membrane Science*, *254*(1–2), 71–79. https://doi.org/10.1016/j.memsci.2004.12.035

Bolton, G., Basha, J., & LaCasse, D. P. (2010). Achieving High Mass-Throughput of Therapeutic Proteins Through Parvovirus Retentive Filters. *Biotechnology Progress*, *26*(6), 1671–1677. https://doi.org/10.1002/btpr.494

Bolton, G., Cabatingan, M., Rubino, M., Lute, S., Brorson, K., & Bailey, M. (2005). Normal-flow virus filtration: detection and assessment of the endpoint in bioprocessing. *Biotechnology and Applied Biochemistry*, *42*(2), 133. https://doi.org/10.1042/BA20050056

Bolton, G., Spector, S., & LaCasse, D. (2006). Increasing the capacity of parvovirus-retentive membranes: performance of the Viresolve™ Prefilter. *Biotechnology and Applied Biochemistry*, *43*(1), 55. https://doi.org/10.1042/BA20050108

Brown, A., Bechtel, C., Bill, J., Liu, H., Liu, J., McDonald, D., Pai, S., Radhamohan, A., Renslow, R., Thayer, B., Yohe, S., & Dowd, C. (2010). Increasing parvovirus filter throughput of monoclonal antibodies using ion exchange membrane adsorptive pre-filtration. *Biotechnology and Bioengineering*, *106*(4), 627–637. https://doi.org/10.1002/bit.22729

Burckbuchler, V., Mekhloufi, G., Giteau, A. P., Grossiord, J. L., Huille, S., & Agnely, F. (2010). Rheological and syringeability properties of highly concentrated human polyclonal immunoglobulin solutions. *European Journal of Pharmaceutics and Biopharmaceutics*, *76*(3), 351–356. https://doi.org/10.1016/j.ejpb.2010.08.002

Buss, N. A., Henderson, S. J., McFarlane, M., Shenton, J. M., & de Haan, L. (2012). Monoclonal antibody therapeutics: history and future. *Current Opinion in Pharmacology*, *12*(5), 615–622. https://doi.org/10.1016/j.coph.2012.08.001

Carter, P. J. (2011). Introduction to current and future protein therapeutics: A protein engineering perspective. *Experimental Cell Research*, *317*(9), 1261–1269. https://doi.org/10.1016/j.yexcr.2011.02.013

Chollangi, S., Parker, R., Singh, N., Li, Y., Borys, M., & Li, Z. (2015). Development of Robust Antibody Purification by Optimizing Protein-A Chromatography in Combination With Precipitation Methodologies. *Biotechnol. Bioeng*, *112*, 2292–2304. https://doi.org/10.1002/bit.25639/abstract

Chon, J. H., & Zarbis-Papastoitsis, G. (2011). Advances in the production and downstream processing of antibodies. *New Biotechnology*, *28*(5), 458–463. https://doi.org/10.1016/j.nbt.2011.03.015

David, L., Niklas, J., Budde, B., Lobedann, M., & Schembecker, G. (2019). Continuous viral filtration for the production of monoclonal antibodies. *Chemical Engineering Research and Design*, *152*, 336–347. https://doi.org/10.1016/j.cherd.2019.09.040

Dimiter, D. (2012). Therapeutic Proteins. In V. Voynov & J. A. Caravella (Eds.), *Methods in Molecular Biology* (second, Vol. 899). Humana Press. https://doi.org/10.1007/978-1-61779-921-1

Dishari, S. K., Venkiteshwaran, A., & Zydney, A. L. (2015). Probing Effects of Pressure Release on Virus Capture During Virus Filtration Using Confocal Microscopy. *Biotechnol. Bioeng*, *112*(10), 2115–2122. https://doi.org/10.1002/bit.25614/abstract

Duhamel, L., Gu, Y., Barnett, G., Tao, Y., Voronov, S., Ding, J., Mussa, N., & Li, Z. J. (2019). Therapeutic protein purity and fragmented species characterization by capillary electrophoresis sodium dodecyl sulfate using systematic hybrid cleavage and forced degradation. *Analytical and Bioanalytical Chemistry*, *411*(21), 5617–5629. https://doi.org/10.1007/s00216-019-01942-8

Dumont, J., Euwart, D., Mei, B., Estes, S., & Kshirsagar, R. (2016). Human cell lines for biopharmaceutical manufacturing: history, status, and future perspectives. *Critical Reviews in Biotechnology*, *36*(6), 1110–1122. https://doi.org/10.3109/07388551.2015.1084266

Emmi, L., & Chiarini, F. (2002). The role of intravenous immunoglobulin therapy in autoimmune and inflammatory disorders. *Neurological Sciences*, *23*(1), S1–S8. https://doi.org/10.1007/s100720200010

Fallahianbijan, F., Emami, P., Hillsley, J. M., Motevalian, S. P., Conde, B. C., Reilly, K., & Zydney, A. L. (2021). Effect of membrane pore structure on fouling behavior of glycoconjugate vaccines. *Journal of Membrane Science*, *619*, 118797. https://doi.org/10.1016/j.memsci.2020.118797

FDA. (1997). *Points to Consider in the Manufacture and Testing of Monoclonal Antibody Products for Human Use*. http://www.fda.gov/cber/cberftp.html

Fekete, S., Beck, A., Veuthey, J.-L., & Guillarme, D. (2014). Theory and practice of size exclusion chromatography for the analysis of protein aggregates. *Journal of Pharmaceutical and Biomedical Analysis*, *101*, 161–173. https://doi.org/10.1016/j.jpba.2014.04.011

Fekete, S., Gassner, A.-L., Rudaz, S., Schappler, J., & Guillarme, D. (2013). Analytical strategies for the characterization of therapeutic monoclonal antibodies. *TrAC Trends in Analytical Chemistry*, *42*, 74–83. https://doi.org/10.1016/j.trac.2012.09.012

Gefroh, E., Dehghani, H., McClure, M., Connell-Crowley, L., & Vedantham, G. (2014). Use of MMV as a single worst-case model virus in viral filter validation studies. *PDA Journal of Pharmaceutical Science and Technology*, *68*(3), 297–311. https://doi.org/10.5731/pdajpst.2014.00978

Giglia, S., & Krishnan, M. (2008). High sensitivity binary gas integrity test for membrane filters. *Journal of Membrane Science*, *323*(1), 60–66. https://doi.org/10.1016/j.memsci.2008.06.017

Goyon, A., D'Atri, V., Bobaly, B., Wagner-Rousset, E., Beck, A., Fekete, S., & Guillarme, D. (2017). Protocols for the analytical characterization of therapeutic monoclonal antibodies. I – Non-denaturing chromatographic techniques. *Journal of Chromatography B*, *1058*, 73–84. https://doi.org/10.1016/j.jchromb.2017.05.010

Han, B., Carlson, J. O., Powers, S. M., & Wickramasinghe, S. R. (2002). Enhanced virus removal by flocculation and microfiltration. *Biotechnology and Bioprocess Engineering*, *7*(1), 6–9. https://doi.org/10.1007/BF02935872

Harris, R. J., Shire, S. J., & Winter, C. (2004). Commercial manufacturing scale formulation and analytical characterization of therapeutic recombinant antibodies. *Drug Development Research*, *61*(3), 137–154. https://doi.org/10.1002/ddr.10344

He, F., Woods, C. E., Becker, G. W., Narhi, L. O., & Razinkov, V. I. (2011). High-Throughput Assessment of Thermal and Colloidal Stability Parameters for Monoclonal Antibody Formulations. *Journal of Pharmaceutical Sciences*, *100*(12), 5126–5141. https://doi.org/10.1002/jps.22712

Howell, J. A., Sanchez, V., & Field, R. W. (1993). *Membranes in Bioprocessing: Theory and Applications*. Springer Netherlands. https://doi.org/10.1007/978-94-011-2156-9

ICH. (1998). *Q5A Viral Safety Evaluation of Biotechnology Products Derived from Cell Lines of Human or Animal Origin*. ICH, Q5A (R1). http://www.fda.gov/cber/guidelines.htm

Ireland, T., Bolton, G., & Noguchi, M. (2005). Optimizing Virus Filter Performance with Prefiltration. *Bioprocess International*, *3*(10), 44–47.

Isu, S. (2022). *Optimizing Virus Filter Performance with Prefiltration* [Graduate Theses and Dissertations, University of Arkansas].

Isu, S., Qian, X., Zydney, A. L., & Wickramasinghe, S. R. (2022). Process- and Product-Related Foulants in Virus Filtration. *Bioengineering*, *9*(4), 155. https://doi.org/10.3390/bioengineering9040155

Jezek, J., Rides, M., Derham, B., Moore, J., Cerasoli, E., Simler, R., & Perez-Ramirez, B. (2011). Viscosity of concentrated therapeutic protein compositions. *Advanced Drug Delivery Reviews*, *63*(13), 1107–1117. https://doi.org/10.1016/j.addr.2011.09.008

Johnson, S. A., Chen, S., Bolton, G., Chen, Q., Lute, S., Fisher, J., & Brorson, K. (2022). Virus filtration: A review of current and future practices in bioprocessing. *Biotechnology and Bioengineering*, *119*(3), 743–761. https://doi.org/10.1002/bit.28017

Johnson, S. A., Walsh, A., Brown, M. R., Lute, S. C., Roush, D. J., Burnham, M. S., & Brorson, K. A. (2017). The step-wise framework to design a chromatography-based hydrophobicity

assay for viral particles. *Journal of Chromatography B, 1061–1062*, 430–437. https://doi.org/10.1016/j.jchromb.2017.08.002

Kahle, J., Zagst, H., Wiesner, R., & Wätzig, H. (2019). Comparative charge-based separation study with various capillary electrophoresis (CE) modes and cation exchange chromatography (CEX) for the analysis of monoclonal antibodies. *Journal of Pharmaceutical and Biomedical Analysis*, *174*, 460–470. https://doi.org/10.1016/j.jpba.2019.05.058

Kamusheva, M., Georgieva, V., Marinov, L., Boncheva, E., Milushewa, P., Grigorova, P., Marinov, K., & Petrova, G. (2021). Volume and trends of adalimumab and pembrolizumab reimbursed market: the Bulgarian perspective. *Biotechnology & Biotechnological Equipment*, *35*(1), 1777–1790. https://doi.org/10.1080/13102818.2021.2019116

Kanani, D. M., Sun, X., & Ghosh, R. (2008). Reversible and irreversible membrane fouling during in-line microfiltration of concentrated protein solutions. *Journal of Membrane Science*, *315*(1–2), 1–10. https://doi.org/10.1016/j.memsci.2008.01.053

Kelley, B. (2007). Very Large Scale Monoclonal Antibody Purification: The Case for Conventional Unit Operations. *Biotechnology Progress*, *23*(5), 995–1008. https://doi.org/10.1021/bp070117s

Kelly, S. T., Senyo Opong, W., & Zydney, A. L. (1993). The influence of protein aggregates on the fouling of microfiltration membranes during stirred cell filtration*. In *Journal of Membrane Science* (Vol. 80).

Kelly, S. T., & Zydney, A. L. (1994). Effects of Intermolecular Thiol-Disulfide Interchange Reactions on BSA Fouling During MicrofiItration. *Biotechnology and Bioengineering*, *44*(8), 972–982. https://doi.org/10.1002/bit.260440814

Kenrick, S., & Some, D. (2014). *The Diffusion Interaction Parameter (kD) as an Indicator of Colloidal and Thermal Stability* (pp. 1–6). Wyatt Technology Corp.

Kern, G., & Krishnan, M. (2006). Virus removal by filtration: points to consider. *BioPharm International*, *19*(10), 32–41.

Kesik-Brodacka, M. (2018). Progress in biopharmaceutical development. *Biotechnology and Applied Biochemistry*, *65*(3), 306–322. https://doi.org/10.1002/bab.1617

Kessler, M., Goldsmith, D., & Schellekens, H. (2006). Immunogenicity of biopharmaceuticals. *Nephrology Dialysis Transplantation*, *21*(suppl_5), v9–v12. https://doi.org/10.1093/ndt/gfl476

King, C., Patel, R., Ponniah, G., Nowak, C., Neill, A., Gu, Z., & Liu, H. (2018). Characterization of recombinant monoclonal antibody variants detected by hydrophobic interaction chromatography and imaged capillary isoelectric focusing electrophoresis. *Journal of Chromatography B*, *1085*, 96–103. https://doi.org/10.1016/j.jchromb.2018.03.049

Kosiol, P., Kahrs, C., Thom, V., Ulbricht, M., & Hansmann, B. (2019). Investigation of virus retention by size exclusion membranes under different flow regimes. *Biotechnology Progress*, *35*(2). https://doi.org/10.1002/btpr.2747

Kueltzo, L. A., Wang, W. E. I., Randolph, T. W., & Carpenter, J. F. (2008). Effects of Solution Conditions, Processing Parameters, and Container Materials on Aggregation of a Monoclonal Antibody during Freeze-Thawing. *Journal of Pharmaceutical Sciences*, *97*(5), 1801–1812. https://doi.org/10.1002/jps.21110

Kunz, W., Henle, J., & Ninham, B. W. (2004). 'Zur Lehre von der Wirkung der Salze' (about the science of the effect of salts): Franz Hofmeister's historical papers. *Current Opinion in Colloid & Interface Science*, *9*(1–2), 19–37. https://doi.org/10.1016/j.cocis.2004.05.005

Leckband, D., & Israelachvili, J. (2001). Intermolecular forces in biology. *Quarterly Reviews of Biophysics*, *34*(2), 105–267. https://doi.org/10.1017/S0033583501003687

Leenaars, M., & Hendriksen, C. F. M. (2005). Critical Steps in the Production of Polyclonal and Monoclonal Antibodies: Evaluation and Recommendations. *ILAR Journal*, *46*(3), 269–279. https://doi.org/10.1093/ilar.46.3.269

Leisi, R., Rostami, I., Laughhunn, A., Bieri, J., Roth, N. J., Widmer, E., & Ros, C. (2022). Visualizing protein fouling and its impact on parvovirus retention within distinct filter membrane morphologies. *Journal of Membrane Science*, *659*, 120791. https://doi.org/10.1016/j.memsci.2022.120791

Li, W., Prabakaran, P., Chen, W., Zhu, Z., Feng, Y., & Dimitrov, D. (2016). Antibody Aggregation: Insights from Sequence and Structure. *Antibodies*, *5*(3), 19. https://doi.org/10.3390/antib5030019

Liu, J. K. H. (2014). The history of monoclonal antibody development – Progress, remaining challenges and future innovations. *Annals of Medicine and Surgery*, *3*(4), 113–116. https://doi.org/10.1016/j.amsu.2014.09.001

Lutz, H., Chang, W., Blandl, T., Ramsey, G., Parella, J., Fisher, J., & Gefroh, E. (2011). Qualification of a novel inline spiking method for virus filter validation. *Biotechnology Progress*, *27*(1), 121–128. https://doi.org/10.1002/btpr.500

Manning, M. C., Chou, D. K., Murphy, B. M., Payne, R. W., & Katayama, D. S. (2010). Stability of Protein Pharmaceuticals: An Update. *Pharmaceutical Research*, *27*, 544–575. https://doi.org/10.1007/s11095-009-0045-6

Marichal-Gallardo, P. A., & Álvarez, M. M. (2012). State-of-the-art in downstream processing of monoclonal antibodies: Process trends in design and validation. *Biotechnology Progress*, *28*(4), 899–916. https://doi.org/10.1002/btpr.1567

McKenzie, E. A., & Abbott, W. M. (2018). Expression of recombinant proteins in insect and mammalian cells. *Methods*, *147*, 40–49. https://doi.org/10.1016/j.ymeth.2018.05.013

Miesegaes, G. R., Lute, S. C., Read, E. K., & Brorson, K. A. (2014). Viral clearance by flow-through mode ion exchange columns and membrane adsorbers. *Biotechnology Progress*, *30*(1), 124–131. https://doi.org/10.1002/btpr.1832

Namila, F. (2020). *The Effects of Solution Condition on Virus Filtration Performance* [Graduate Theses and Dissertations, University of Arkansas]. https://scholarworks.uark.edu/etd/3892

Namila, F., Zhang, D., Traylor, S., Nguyen, T., Singh, N., Wickramasinghe, R., & Qian, X. (2019). The effects of buffer condition on the fouling behavior of MVM virus filtration of an Fc-fusion protein. *Biotechnology and Bioengineering*, *116*(10), 2621–2631. https://doi.org/10.1002/bit.27085

Nielsen, E. (2022). *Small Scale Monoclonal Antibody Purification Platform* [Graduate Theses , Lund University]. www.chemeng.lth.se

Nissim, A., & Chernajovsky, Y. (2008). Historical Development of Monoclonal Antibody Therapeutics. In *Therapeutic antibodies* (Vol. 181, pp. 3–18).

Nobbmann, U., Connah, M., Fish, B., Varley, P., Gee, C., Mulot, S., Chen, J., Zhou, L., Lu, Y., Sheng, F., Yi, J., & Harding, S. E. (2007). Dynamic light scattering as a relative tool for assessing the molecular integrity and stability of monoclonal antibodies. *Biotechnology and Genetic Engineering Reviews*, *24*(1), 117–128. https://doi.org/10.1080/02648725.2007.10648095

Novák, P., & Havlíček, V. (2016). Protein Extraction and Precipitation. In *Proteomic Profiling and Analytical Chemistry* (pp. 51–62). Elsevier. https://doi.org/10.1016/B978-0-444-63688-1.00004-5

Owczarek, B., Gerszberg, A., & Hnatuszko-Konka, K. (2019). A Brief Reminder of Systems of Production and Chromatography-Based Recovery of Recombinant Protein Biopharmaceuticals. *Biomed Res Int*, *2019*, 1–13. https://doi.org/10.1155/2019/4216060

Papathanasiou, M. M., Quiroga-Campano, A. L., Steinebach, F., Elviro, M., Mantalaris, A., & Pistikopoulos, E. N. (2017). Advanced model-based control strategies for the intensification of upstream and downstream processing in mAb production. *Biotechnology Progress*, *33*(4), 966–988. https://doi.org/10.1002/btpr.2483

Philo, J., & Arakawa, T. (2009). Mechanisms of Protein Aggregation. *Current Pharmaceutical Biotechnology*, *10*(4), 348–351. https://doi.org/10.2174/138920109788488932

Puetz, J., & Wurm, F. M. (2019). Recombinant proteins for industrial versus pharmaceutical purposes: a review of process and pricing. *Processes*. https://doi.org/10.3390/pr7080476

Rao, S., Gefroh, E., & Kaltenbrunner, O. (2012). Recovery modeling of tangential flow systems. *Biotechnology and Bioengineering*, *109*(12), 3084–3092. https://doi.org/10.1002/bit.24577

Rayfield, W. J., Roush, D. J., Chmielowski, R. A., Tugcu, N., Barakat, S., & Cheung, J. K. (2015). Prediction of Viral Filtration Performance of Monoclonal Antibodies Based on

Biophysical Properties of Feed. *Biotechnology Progress*, *31*(3), 765–774. https://doi.org/10.1002/btpr.2094

Reichert, J. M. (2008). Monoclonal Antibodies as Innovative Therapeutics. *Current Pharmaceutical Biotechnology*, *9*(6), 423–430. https://doi.org/10.2174/138920108786786358

Reichert, J. M. (2013). Monoclonal antibodies in drug and vaccine development. *Drug Discovery Today*.

Reichert, J. M., & Valge-Archer, V. E. (2007). Development trends for monoclonal antibody cancer therapeutics. *Nature Reviews Drug Discovery*, *6*(5), 349–356. https://doi.org/10.1038/nrd2241

Robinson, J., Roush, D., & Cramer, S. (2018). Domain contributions to antibody retention in multimodal chromatography systems. *Journal of Chromatography A*, *1563*, 89–98. https://doi.org/10.1016/j.chroma.2018.05.058

Rosenberg. (2006). Effects of protein aggregates: An immunologic perspective. *The AAPS Journal*, *8*(3), E501–E507. https://doi.org/10.1208/aapsj080359

Rosenberg. (2010). *Aggregation of Therapeutic Antibodies in the Course of Downstream Processing vorgelegt von* [Graduate Theses and Dissertations]. lmu.

Rosenberg, A. S., Verthelyi, D., & Cherney, B. W. (2012). Managing uncertainty: A perspective on risk pertaining to product quality attributes as they bear on immunogenicity of therapeutic proteins. *Journal of Pharmaceutical Sciences*, *101*(10), 3560–3567. https://doi.org/10.1002/jps.23244

Roth, N. J., Dichtelmüller, H. O., Fabbrizzi, F., Flechsig, E., Gröner, A., Gustafson, M., Jorquera, J. I., Kreil, T. R., Misztela, D., Moretti, E., Moscardini, M., Poelsler, G., More, J., Roberts, P., Wieser, A., & Gajardo, R. (2020). Nanofiltration as a robust method contributing to viral safety of plasma-derived therapeutics: 20 years' experience of the plasma protein manufacturers. *Transfusion*, *60*(11), 2661–2674. https://doi.org/10.1111/trf.16022

Rustandi, R. R., Washabaugh, M. W., & Wang, Y. (2008). Applications of CE SDS gel in development of biopharmaceutical antibody-based products. *ELECTROPHORESIS*, *29*(17), 3612–3620. https://doi.org/10.1002/elps.200700958

Saluja, A., Fesinmeyer, R. M., Hogan, S., Brems, D. N., & Gokarn, Y. R. (2010). Diffusion and Sedimentation Interaction Parameters for Measuring the Second Virial Coefficient and Their Utility as Predictors of Protein Aggregation. *Biophysical Journal*, *99*(8), 2657–2665. https://doi.org/10.1016/j.bpj.2010.08.020

Saxena, A., Tripathi, B. P., Kumar, M., & Shahi, V. K. (2009). Membrane-based techniques for the separation and purification of proteins: An overview. *Advances in Colloid and Interface Science*, *145*(1–2), 1–22. https://doi.org/10.1016/j.cis.2008.07.004

Shieh, I. C., & Patel, A. R. (2015). Predicting the Agitation-Induced Aggregation of Monoclonal Antibodies Using Surface Tensiometry. *Molecular Pharmaceutics*, *12*(9), 3184–3193. https://doi.org/10.1021/acs.molpharmaceut.5b00089

Shinoda, T., Shinya, N., Ito, K., Ishizuka-Katsura, Y., Ohsawa, N., Terada, T., Hirata, K., Kawano, Y., Yamamoto, M., Tomita, T., Ishibashi, Y., Hirabayashi, Y., Kimura-Someya, T., Shirouzu, M., & Yokoyama, S. (2016). Cell-free methods to produce structurally intact mammalian membrane proteins OPEN. *Nature: Scientific Reports*. https://doi.org/10.1038/srep30442

Shire, S. J., Shahrokh, Z., & Liu, J. (2004). Challenges in the development of high protein concentration formulations. *Journal of Pharmaceutical Sciences*, *93*(6), 1390–1402. https://doi.org/10.1002/jps.20079

Singh, S. K., Afonina, N., Awwad, M., Bechtold-Peters, K., Blue, J. T., Chou, D., Cromwell, M., Krause, H.-J., Mahler, H.-C., Meyer, B. K., Narhi, L., Nesta, D. P., & Spitznagel, T. (2010). An Industry Perspective on the Monitoring of Subvisible Particles as a Quality Attribute for Protein Therapeutics. *Journal of Pharmaceutical Sciences*, *99*(8), 3302–3321. https://doi.org/10.1002/jps.22097

Sofer, G., Brorson, K., Abujoub, A., Aranha, H., Burnouf, T., Carter, J., Jocham, U. E., Jornitz, M., Korneyeva, M., Krishnan, M., Marcus-Sekura, C., Martin, J., Morgan, M., Prashad, M., Robertson, G. A., Rubino, M., Shanks, M., Shepherd, A., Smith, T., … Yoshinari, K. B. (2005). PDA Technical Report No. 41 : Virus filtration. *PDA Journal of Pharmaceutical Science and Technology*, *59*(SUPPL. 2), 1–42.

Sommerfeld, S., & Strube, J. (2005). Challenges in biotechnology production—generic processes and process optimization for monoclonal antibodies. *Chemical Engineering and Processing: Process Intensification*, *44*(10), 1123–1137. https://doi.org/10.1016/j.cep.2005.03.006

Stanevich, V., Pachalla, A., Nunez, B., McInnes, M., Nieder, C., & Schreffler, J. (2021). Improving viral filtration capacity in biomanufacturing processes using aggregate binding properties of polyamide-6,6. *Biotechnology and Bioengineering*, *118*(3), 1105–1115. https://doi.org/10.1002/bit.27634

Syedain, Z. H., Bohonak, D. M., & Zydney, A. L. (2006). Protein Fouling of Virus Filtration Membranes: Effects of Membrane Orientation and Operating Conditions. *Biotechnology Progress*, *22*(4), 1163–1169. https://doi.org/10.1021/bp050350v

Thiagarajan, G., Semple, A., James, J. K., Cheung, J. K., & Shameem, M. (2016). A comparison of biophysical characterization techniques in predicting monoclonal antibody stability. *MAbs*, *8*(6), 1088–1097. https://doi.org/10.1080/19420862.2016.1189048

Tripathi, N. K., & Shrivastava, A. (2019). Recent Developments in Bioprocessing of Recombinant Proteins: Expression Hosts and Process Development. *Front Bioeng Biotechnol*, *7*, 420. https://doi.org/10.3389/fbioe.2019.00420

Troccoli, N. M., Mciver, J., Losikoff, A., & Poiley, J. (1998). Removal of Viruses from Human Intravenous Immune Globulin by 35 nm Nanofiltration. *Biologicals*, *26*, 321–329.

van Reis, R., & Zydney, A. (2007). Bioprocess membrane technology. *Journal of Membrane Science*, *297*(1–2), 16–50. https://doi.org/10.1016/j.memsci.2007.02.045

Vázquez-Rey, M., & Lang, D. A. (2011). Aggregates in monoclonal antibody manufacturing processes. *Biotechnology and Bioengineering*, *108*(7), 1494–1508. https://doi.org/10.1002/bit.23155

Wagner, E., Colas, O., Chenu, S., Goyon, A., Murisier, A., Cianferani, S., François, Y., Fekete, S., Guillarme, D., D'Atri, V., & Beck, A. (2020). Determination of size variants by CE-SDS for approved therapeutic antibodies: Key implications of subclasses and light chain specificities. *Journal of Pharmaceutical and Biomedical Analysis*, *184*, 113166. https://doi.org/10.1016/j.jpba.2020.113166

Wang, W. (2005). Protein aggregation and its inhibition in biopharmaceutics. *International Journal of Pharmaceutics*, *289*(1–2), 1–30. https://doi.org/10.1016/j.ijpharm.2004.11.014

Wickramasighe, S. R., Namila, F., & Qian, X. (2019). Virus Removal and Virus Purification. *In Current Trends and Future Developments on (Bio-) Membranes; Elsevier: Amsterdam, The Netherlands*, 69–96. https://doi.org/10.1016/B978-0-12-813606-5.00003-8

Wickramasinghe, S. R., Stump, E. D., Grzenia, D. L., Husson, S. M., & Pellegrino, J. (2010). Understanding virus filtration membrane performance. *Journal of Membrane Science*, *365*(1–2), 160–169. https://doi.org/10.1016/j.memsci.2010.09.002

Wiesner, R., Scheller, C., Krebs, F., Wätzig, H., & Oltmann-Norden, I. (2021). A comparative study of CE-SDS, SDS-PAGE, and Simple Western: Influences of sample preparation on molecular weight determination of proteins. *ELECTROPHORESIS*, *42*(3), 206–218. https://doi.org/10.1002/elps.202000199

Willkommen, H., BluMel, J., Brorson, K., Chen, D., Chen, Q., GroNer, A., Kreil, T. R., Robertson, J. S., Ruffing, M., & Ruiz, S. (2013). Meeting Report--Workshop on Virus Removal by Filtration: Trends and New Developments. *PDA Journal of Pharmaceutical Science and Technology*, *67*(2), 98–104. https://doi.org/10.5731/pdajpst.2013.00907

Winter, G., Griffiths, A. D., Hawkins, R. E., & Hoogenboom, H. R. (1994). Making Antibodies by Phage Display Technology. *Annual Review of Immunology*, *12*(1), 433–455. https://doi.org/10.1146/annurev.iy.12.040194.002245

Wöll, A. K., & Hubbuch, J. (2020). Investigation of the reversibility of freeze/thaw stress-induced protein instability using heat cycling as a function of different cryoprotectants. *Bioprocess and Biosystems Engineering*, *43*(7), 1309–1327. https://doi.org/10.1007/s00449-020-02327-3

Woods, M. A., & Zydney, A. L. (2014). Effects of a pressure release on virus retention with the Ultipor DV20 membrane. *Biotechnology and Bioengineering*, *111*(3), 545–551. https://doi.org/10.1002/bit.25112

Yadav, S., Shire, S. J., & Kalonia, D. S. (2010). Factors Affecting the Viscosity in High Concentration Solutions of Different Monoclonal Antibodies. *Journal of Pharmaceutical Sciences*, *99*(12), 4812–4829. https://doi.org/10.1002/jps.22190

Yigzaw, Y., Hinckley, P., Hewig, A., & Vedantham, G. (2009). Ion Exchange Chromatography of Proteins and Clearance of Aggregates. *Current Pharmaceutical Biotechnology*, *10*(4), 421–426. https://doi.org/10.2174/138920109788488842

Zhang, Y., Wang, Y., & Li, Y. (2019). A method for improving protein A chromatography's aggregate removal capability. *Protein Expression and Purification*, *158*, 65–73. https://doi.org/10.1016/j.pep.2019.02.017

Zydney, A. L. (2009). Membrane technology for purification of therapeutic proteins. *Biotechnology and Bioengineering*, *103*(2), 227–230. https://doi.org/10.1002/bit.22308